

A hydromechanical and biochemical model of stomatal conductance

T. N. BUCKLEY¹, K. A. MOTT² & G. D. FARQUHAR¹

¹Environmental Biology Group and Cooperative Research Centre for Greenhouse Accounting, Research School of Biological Sciences, The Australian National University, GPO Box 475, Canberra City, ACT 2601, Australia and ²Department of Biology, Utah State University, Logan, UT 84322–5305, USA

ABSTRACT

A mathematical model of stomatal conductance is presented. It is based on whole-plant and epidermal hydromechanics, and on two hypotheses: (1) the osmotic gradient across guard cell membranes is proportional to the concentration of ATP in the guard cells; and (2) the osmotic gradient that can be sustained per unit of ATP is proportional to the turgor pressure of adjacent epidermal cells. In the present study, guard cell [ATP] is calculated using a previously published model that is based on a widely used biochemical model of C₃ mesophyll photosynthesis. The conductance model for *Vicia faba* L. is parameterized and tested. As with most other stomatal models, the present model correctly predicts the stomatal responses to variations in transpiration rate, irradiance and intercellular CO₂. Unlike most other models, however, this model can predict the transient stomatal opening often observed before conductance declines in response to decreases in humidity, soil water potential, or xylem conductance. The model also explicitly accommodates the mechanical advantage of the epidermis and correctly predicts that stomata are relatively insensitive to the ambient partial pressure of oxygen, as a result of the assumed dependence on ATP concentration.

Key-words: gas exchange; guard cell; photosynthesis; stomata; transpiration.

INTRODUCTION

A model of stomatal conductance (g_{sw} or simply g ; see Table 1 for a list of symbols) is required to predict plant gas exchange accurately. Most models of leaf and canopy gas exchange use a phenomenological model for g (e.g. Jarvis 1976; Ball, Woodrow & Berry 1987; the latter modified by Leuning 1995; and more recently by Tuzet, Perrier & Leuning 2003). These models have been successful because they are mathematically simple, and because they agree with direct measurements of g under many conditions. However, it is difficult to interpret their mathematical structures in terms of the regulatory mechanisms that they presumably

mimic. This limits their usefulness as tools for probing stomatal and leaf functioning and constrains the confidence with which their predictions can be extended to future climates. To address these limitations, several authors have attempted recently to model g in a more mechanistically explicit fashion (e.g. Dewar 2002; Gao *et al.* 2002). However, those models were based on assumptions about epidermal water relations and stomatal hydromechanics that are inconsistent with recent experiments and they calculated guard cell osmotic pressure (π_g) from irradiance or photosynthetic variables in a phenomenological fashion, much like the Jarvis and Ball–Berry models (Jarvis 1976; Ball *et al.* 1987) discussed above. Our goal was to develop and present a model for g that overcomes some of these limitations.

Many stomatal responses are driven by changes in π_g , which is determined partly by solute influx in response to a proton-motive force created by plasma membrane H⁺-ATPases (e.g. Tominaga, Kinoshita & Shimazaki 2001). Although this is a well-established paradigm in stomatal physiology, it is rarely incorporated explicitly into models of stomatal conductance. One of the few attempts to do so (Farquhar & Wong 1984) assumed that g itself, rather than π_g , is proportional to the concentration of ATP in photosynthetic cells, which could be calculated from the biochemical photosynthesis model developed by Farquhar, Caemmerer & Berry (1980). That conductance model predicted observed responses to irradiance, temperature, CO₂ partial pressure, O₂ partial pressure and leaf chlorophyll content. However, it could not predict any response to hydraulic factors such as humidity or water supply to the leaf, because it did not explicitly include the hydromechanical context that links guard cell osmotic pressure to stomatal conductance. A single value of π_g can produce a wide range of stomatal apertures and conductances, depending on the relationships between guard cell turgor pressure and volume, between guard and epidermal cell water potentials and between stomatal aperture and guard and epidermal cell turgor pressures.

Intensive study of these hydromechanical factors reveals a paradox. When the rate of water loss from the leaf is experimentally increased (for example, by decreasing ambient humidity), leaf turgor and stomatal aperture both decline in the steady state (Shackel & Brinkmann 1985; Monteith 1995; Mott & Franks 2001). However, pressure

Correspondence: T. N. Buckley. E-mail: tom_buckley@alumini.jmu.edu.

Table 1. Mathematical terms used in this paper

Name	Symbol	Value	Units
Terms in the model (Eqn 6)			
Stomatal conductance to water vapour	g_{sw}, g	–	mol air m ⁻² s ⁻¹
ATP concentration	τ	–	mmol ATP m ⁻²
Hydromechanical/biochemical response parameter	β	1.17 ± 0.27 ^b	[mmol ATP m ⁻²] ⁻¹
Residual epidermal mechanical advantage	M	0.98 ^b	unitless
Guard cell resistive advantage	ρ	0 ^a	unitless
Effective hydraulic resistance to the epidermis	R	0.0456 ^b	MPa [mmol H ₂ O m ⁻² s ⁻¹] ⁻¹
Epidermal osmotic pressure	π_e	0.525 ^b	MPa
Apoplastic osmotic pressure	π_a	0 ^a	MPa
Leaf-to boundary layer H ₂ O mole fraction gradient	D_s	10 [5–30]	mmol H ₂ O mol ⁻¹ air
Source water potential	ψ_s	0 ^a	MPa
Turgor-to-conductance scaling factor	χ	0.105 ^b	mol air m ⁻² s ⁻¹ MPa ⁻¹
Terms in simplified form of the model (Eqn 7)			
Guard cell advantage	α	–	unitless
ATP-saturated stomatal conductance	g_m	–	mol air m ⁻² s ⁻¹
'Michaelis constant' for α	K_g	–	unitless
Hydroactive compensation point	γ	–	unitless
Other terms in the model derivation			
Epidermal mechanical advantage [fitted value]	$m [\hat{m}]$	1.98 ^b	unitless
Guard cell osmotic pressure	π_g	–	MPa
Water potential of z	ψ_z	–	MPa
Turgor pressure of z	P_z	–	MPa
Resistance from y to z	r_{yz}	–	MPa [mmol H ₂ O m ⁻² s ⁻¹] ⁻¹
Effective hydraulic resistance to the guard cells	R_g	–	MPa [mmol H ₂ O m ⁻² s ⁻¹] ⁻¹
Fraction of transpiration that occurs from z	f_z	–	unitless
Leaf transpiration rate	E	–	mmol H ₂ O m ⁻² s ⁻¹
Boundary layer resistance to water vapour	r_{bw}	–	[mol air m ⁻² s ⁻¹] ⁻¹
Terms in the ATP submodel			
Leaf net CO ₂ assimilation rate	A	–	μ mol CO ₂ m ⁻² s ⁻¹
Rate of respiration that continues in the dark	R_d	–	μ mol CO ₂ m ⁻² s ⁻¹
Photorespiratory CO ₂ compensation point	Γ^*	–	Pa
Intercellular CO ₂ partial pressure	p_i	–	Pa
Michaelis constant for RuBP carboxylation	K_c	40.4 ^c	Pa
Michaelis constant for RuBP oxygenation	K_o	2.48 × 10 ^{3c}	Pa
Light-limited potential electron transport rate	J	–	μ mol e ⁻ m ⁻² s ⁻¹
Light-saturated potential electron transport rate	J_m	(2.02 ± 0.48) · V _m ^b	μ mol e ⁻ m ⁻² s ⁻¹
Curvature parameter for $J(I, J_m)$	θ_j	0.908 ± 0.030 ^b	unitless
Incident photosynthetically active irradiance	I	1100 [50–1600]	μ mol photons m ⁻² s ⁻¹
Product of absorbance and effective quantum yield	F	0.195 ± 0.020 ^b	electrons photon ⁻¹
Ambient O ₂ partial pressure	p_{O_2}	(2.10 [0.2–4]) × 10 ³	Pa
Ambient CO ₂ concentration	c_a	365 [50–1000]	p.p.m.
Atmospheric pressure	p_t	10 ^{5 a}	Pa
ATP concentration	τ	–	mmol ATP m ⁻²
ATP concentration when $W_c > W_j$	τ_j	–	mmol ATP m ⁻²
ATP concentration when $W_j > W_c$	τ_c	–	mmol ATP m ⁻²
Basal ATP level provided by other processes	τ_o	1.6 ^a	mmol ATP m ⁻²
Total concentration of adenylates ($\tau + [ADP]$)	a_t	12.6 · V _m ^d	mmol AxP m ⁻²
Concentration of photophosphorylation sites	p	2.5 · V _m ^d	mmol sites m ⁻²
Potential RuBP pool size	R_p	–	μ mol RuBP m ⁻²
Total concentration of Rubisco active sites	E_t	–	μ mol sites m ⁻²
Rubisco turnover number	k_c	–	CO ₂ site ⁻¹ s ⁻¹
Carboxylation rate:			
Limited by CO ₂ and Rubisco, but not by RuBP	W_c	–	μ mol CO ₂ m ⁻² s ⁻¹
Limited by RuBP and CO ₂ , but not by Rubisco	W_j	–	μ mol CO ₂ m ⁻² s ⁻¹
Limited by Rubisco only	V_m	(8.86 ± 0.215) × 10 ^{1b}	μ mol CO ₂ m ⁻² s ⁻¹
Limited by potential RuBP pool size only	V_r	2.27 · V _m ^d	μ mol CO ₂ m ⁻² s ⁻¹

Values are given where appropriate; where ranges are given in brackets, standard values are given in italics, and for parameters estimated by gas exchange, standard deviations are given, preceded by the ± symbol. Sources: ^aassumption; ^bAppendix 4; ^cCaemmerer *et al.* (1994); ^dFarquhar & Wong (1984). The notation |V_m| means the numerical value of V_m, i.e. V_m/[μ mol CO₂ m⁻² s⁻¹]. The subscripts _z and _y are placeholders for e, g, x, or m, referring to epidermal cells, guard cells, xylem, and mesophyll cells, respectively. Where experimental precision was known, non-significant digits are subscripted but retained for accuracy.

probe experiments suggest that equal reductions in guard cell and epidermal turgor should cause stomatal aperture to *increase*; this is because aperture responds negatively, and more strongly, to the ‘backpressure’ of epidermal cells than to the opening force provided by guard cell turgor (Franks, Cowan & Farquhar 1998). Therefore, guard and epidermal cell turgors must be decoupled from one another during the steady-state response of g to changes in hydraulic supply and demand (Buckley & Mott 2002a). Two principal hypotheses have been advanced to explain this decoupling. The first, which we call the ‘metabolic regulation hypothesis’, suggests that π_g is actively regulated in proportion to the water potential or turgor pressure of cells near the evaporating site (Haefner, Buckley & Mott 1997). The second, which we call the ‘drawdown hypothesis’, suggests that steady-state stomatal responses to hydraulic perturbations are caused by a water potential gradient from epidermal to guard cells (Dewar 1995, 2002).

Each of these hypotheses can explain the steady-state humidity response. However, to explain both the transient and steady-state phases of the humidity response, the drawdown hypothesis requires the hydraulic conductivity from epidermal to guard cells to vary with VPD in complex fashion (Buckley & Mott 2002a), but there is neither any established role in stomatal behaviour for cell-to-cell conductivity regulation, nor any proven mechanism to effect such regulation. In contrast, the metabolic regulation hypothesis is based on a simple, monotonic relationship between π_g and P_e , both in the steady-state and transient phases of the humidity response, and it predicts a monotonic steady-state relationship between π_g and VPD (Buckley & Mott 2002a). For these reasons, and because it explains short-term hydraulic responses in terms of the same mechanism – osmotic regulation – that drives most other stomatal responses, the metabolic regulation hypothesis seems most parsimonious.

In this study, we derive a closed-form model of g based on two hypotheses: (1) the osmotic gradient across guard cell membranes, $\delta\pi_g$, is limited by guard cell ATP concentration, τ ; and (2) the osmotic gradient that can be sustained per unit of ATP is proportional to epidermal turgor pressure, P_e (the metabolic regulation hypothesis). We simulate τ in the present study using the model of Farquhar & Wong (1984) for [ATP] in C_3 mesophyll cells, which is based on the model of Farquhar *et al.* (1980) for C_3 mesophyll photosynthesis. The use of that ATP submodel entails the implicit assumption that similar biochemical processes control [ATP] in guard cells and in mesophyll cells; however, the model’s validity does not rest on this assumption, and requires merely that [ATP] respond to environmental factors as required to produce observed conductance responses. We assume that stomatal aperture is determined by guard and epidermal cell turgor pressures in the manner shown by Franks *et al.* (1995, 1998). We parameterize and test the stomatal model for *Vicia faba* L., interpret its behaviour with the help of some algebraic simplifications, and discuss its structure and behaviour in relation to other stomatal models.

SYNOPSIS OF THE MODELLING APPROACH

Our model, like several other recent efforts (Dewar 1995, 2002; Haefner *et al.* 1997; Gao *et al.* 2002), is based on five assertions that form a mathematical ‘closed loop.’ These are: (1) stomatal conductance is proportional to stomatal aperture ($g \propto a$); (2) aperture is controlled by guard cell turgor pressure ($a \propto P_g$); (3) turgor is the sum of water potential and osmotic pressure ($P_g = \psi_g + \pi_g$); (4) water potential is ‘drawn down’ to guard cells from a source and through a resistance, by transpiration ($\psi_g = \psi_s - ER_g$) (Fig. 1 shows a resistance diagram); and (5) transpiration rate is the product of conductance and evaporative gradient ($E = gD_s$). Combining the first two assertions as $g = \chi P_g$ (with χ a constant), the solution of these equations (derived as Eqn A7 in Appendix 1) is

$$g = \chi \frac{\psi_s + \pi_g}{1 + \chi R_g D_s} \quad (1)^\circ$$

[The symbol $^\circ$, which also appears on Eqn 4 below, indicates that this expression is *not* part of our model – it is presented only for heuristic purposes.] Equation 1 is consistent with the observation that stomata open more in well-watered

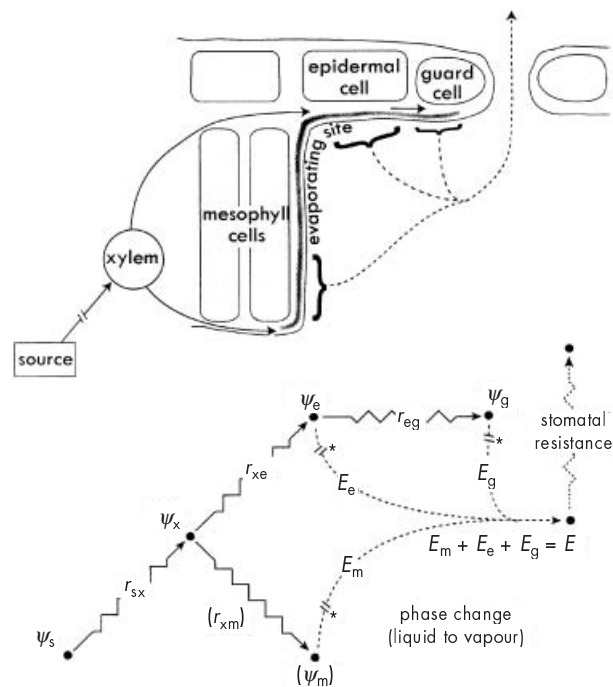


Figure 1. Diagrams illustrating the hydraulic structure of the model. Evaporation sites are distributed continuously from near the inner walls of the guard cells to the mesophyll cells, and our model discretizes this continuum into three distinct sites: guard, epidermis, and mesophyll. These three evaporation fractions must sum to unity. However, the mesophyll cell water potential (ψ_m) and the resistance from the xylem to the mesophyll (r_{xm}) do not explicitly appear in our model, so they are shown in parentheses. Note that stomatal resistance is *not* commensurable with the liquid-phase resistances, because of the phase change from liquid to vapour.

plants (high ψ_s), less in dry air (high D_s) and less under high hydraulic resistance (R_g), and that stomatal opening in the light is accompanied by an increase in guard cell osmotic pressure. This expression is the hydromechanical framework of the model of Gao *et al.* (2002). It contains a single negative hydraulic feedback loop (loop no. 1 in Fig. 2a), formed by the assertions underlying Eqn 1: an increase in g decreases ψ , which lowers P , reducing stomatal aperture and thus g . This feedback loop is what causes the steady-state responses to D_s , ψ_s and R_g in Eqn 1 and in the Gao model.

However, Eqn 1 does not account for the effect of epidermal turgor pressure, P_e , on aperture. Theoretical analysis and pressure probe experiments (DeMichele & Sharpe 1973; Edwards, Meidner & Sheriff 1976; Sharpe, Wu & Spence 1987; Franks *et al.* 1998) show that stomatal aperture responds positively to guard cell turgor pressure (P_g), but negatively, and more strongly, to epidermal cell turgor (P_e). Thus, the assertion that $g = \chi P_g$ is replaced by

$$g = \chi(P_g - \hat{m}P_e), \hat{m} > 1 \quad (2)$$

The parameter ' \hat{m} ' is often termed the 'mechanical advantage' of the epidermis and $M \equiv \hat{m} - 1$ is the 'residual' mechanical advantage. The observation that $\hat{m} > 1$ ($M > 0$) creates some complications: (1) guard cells are 'downstream' from epidermal cells in the transpiration stream, so they may have a lower water potential than epidermal cells ($\psi_g < \psi_e$) and support a different fraction of transpiration (f_g); (2) the hydraulic resistance for water flow to guard cells (R_g) may be higher than that for the epidermis (R), so $R_g = R + f_g r_{eg}$ (see resistance diagram in Fig. 1); and (3) guard and epidermal cells may also have different osmotic pressures ($\pi_g > \pi_e$ generally). When these features are added to the assertions underlying Eqn 1, the solution (derived as Eqn A10 in Appendix 1) is

$$g = \chi \frac{-M(\psi_s + \pi_e) + \pi_g - \pi_e}{1 - \chi R D_s (M - f_g r_{eg}/R)}, (M \equiv \hat{m} - 1) \quad (3)$$

Despite being more complicated than Eqn 1, this expression seems incorrect at first glance, because the response to source water potential is now negative, and if $M > f_g r_{eg}/R$, the responses to hydraulic resistance and humidity are also in the wrong direction. This occurs because the positive feedback that operates via P_e (loop no. 2 in Fig. 2a) is stronger than the negative feedback via P_g (loop no. 1 in Fig. 2a) because $m > 1$.

Dewar (2002) suggested a resolution to this problem. He noted that M could be considered zero if one interprets P_e as the 'bulk' epidermal turgor (averaged over all epidermal cells, not only the 'subsidiary' cells that immediately adjoin the guard cells), and if π_e is lower in non-subsidiary than in subsidiary epidermal cells. If the postulated difference between π_e and ' $\pi_{e,bulk}$ ' is large enough to overcome the mechanical advantage of the subsidiary cells and the increase in water potential that should occur with distance from each stomatal pore, then Eqn 2 can be replaced by

$g = \chi(P_g - P_{e,bulk})$, implying $M = 0$. Applied to Eqn 3, this yields a new solution (Eqn A11 in Appendix 1):

$$g = \chi \frac{\pi_g - \pi_{e,bulk}}{1 + \chi f_g r_{eg} D_s} \quad (4)^\circ$$

[The $^\circ$ symbol indicates this is *not* part of our model, as for Eqn 1.] By nullifying the mechanical advantage, the Dewar resolution weakens the positive hydraulic feedback that occurs via P_e , making its intrinsic strength equal to that of the negative feedback via P_g . The negative feedback is then strengthened by a hydraulic gradient from epidermal to guard cells, equal to $f_g r_{eg} D_s$. This resolution produces the correct negative steady-state response to D_s , but by focusing direct hydraulic responses in the epidermal-to-guard cell gradient, it eliminates the direct effects of ψ_s and R – necessitating an additional model to predict stomatal responses to those factors. Dewar (2002) used a soil–plant hydraulic model to calculate epidermal water potential (ψ_e) and then postulated an effect of ψ_e on the sensitivity of guard cell solute leakage to xylem sap ABA. To produce observed responses to intercellular CO_2 concentration (c_i) and irradiance, Dewar assumed π_g was proportional to the rate of gross photosynthesis, and inversely proportional to c_i ; these effects correspond to feedback loop no. 4 in Fig. 2a.

However, the core assumption underlying Eqn 4 is called into question by pressure probe experiments that found no systematic variation in turgor between subsidiary and non-subsidiary epidermal cells (Franks *et al.* 1995, 1998; Mott & Franks 2001). Additionally, it is often observed that stomata *initially* respond in the 'wrong direction' when ψ_s , R or D_s are varied and then reverse course and slowly converge to the 'correct' steady-state response. Equation 4 does not predict these 'wrong-way' responses, whereas Eqn 3 does.

A different resolution

We accept at face value the experimental evidence suggesting that $M > 0$ ($\hat{m} > 1$ in Eqn 2), regardless of where in the epidermis P_e is measured. As a result, the net hydropassive feedback that results from a change in D_s , ψ_s , or R is positive, because the mechanical advantage renders the hydropassive feedback through P_e (loop no. 2 in Fig. 2a) stronger than that via P_g (loop no. 1 in Fig. 2a). Buckley & Mott (2002a, b) proposed a resolution that avoids the need to assume a spatial gradient in π_e or a large value of $f_g r_{eg}$, and that predicts both the steady-state and temporary 'wrong-way' responses to D_s , ψ_s and R with a single mechanism. Below, we formalize that resolution and use it to derive a new steady-state model of stomatal conductance.

Specifically, we hypothesize that the steady-state osmotic gradient across guard cell membranes ($\delta\pi_g$) is proportional to guard cell ATP concentration, τ , and that the sensitivity of $\delta\pi_g$ to τ scales with epidermal turgor pressure, P_e . These hypotheses create another feedback loop that operates via P_e (loop no. 3 in Fig. 2a), but which has negative gain. This negative, *hydroactive* feedback gradually overrides the initial positive *hydropassive* feedback caused by the mechanical advantage, so that *at steady state*,

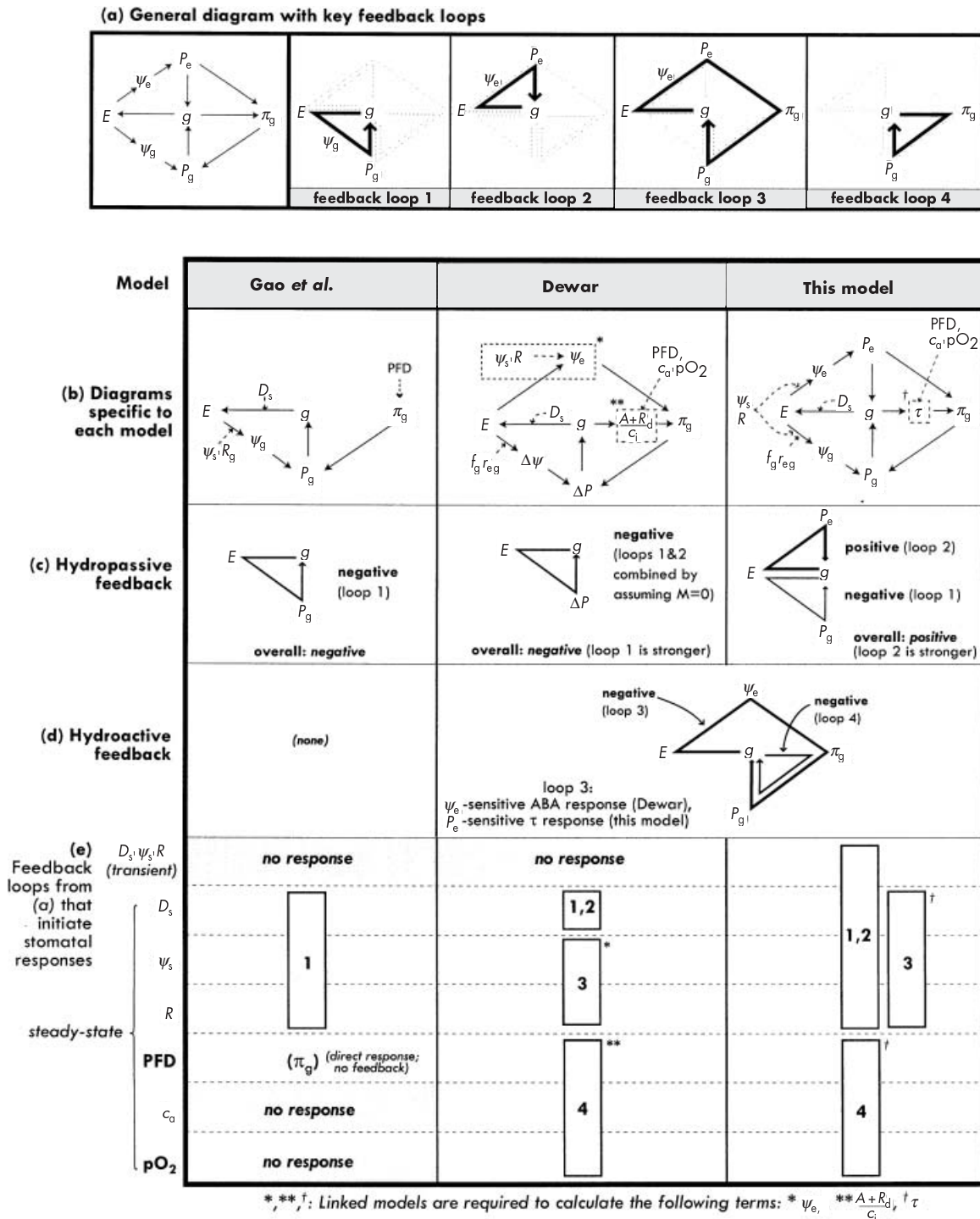


Figure 2. Diagrams showing influences among key variables in three recent hydromechanical models of stomatal conductance (Gao *et al.* 2002; Dewar 2002; and the model presented in this study). (a) Generic diagram with four important feedback loops highlighted and numbered from 1 to 4. (b) Diagrams of each model, modified from the generic diagram, and showing where each of six stomatal effectors (D_s , ψ_s , R , c_a , PFD and pO_2) influences the system directly. (c) Feedbacks in each model that are purely physical or hydraulic feedbacks (hydropassive). In the Dewar model, the assumption that $M = 0$ collapses loops no. 1 and no. 2 into one term, ΔP ($P_g - P_e$), which then uniquely determines aperture. The resulting combined feedback loop has negative gain because any resistance from epidermal to guard cells ($f_g r_{eg}$) causes P_g to decrease more than P_e when E increases. In our model, the mechanical advantage makes the loop no. 2 stronger than loop no. 1, so the net hydropassive feedback is positive. (d) Feedbacks with a biochemical component. The Dewar model uses loop no. 3 to produce responses to ψ_e and R ; our model uses loop no. 3 to override the positive hydropassive feedback shown in (c). Both models also include negative feedback from the photosynthetic apparatus (loop no. 4). (e) Major stomatal responses (listed on the left) and the feedback loops, numbered as in (a), that are responsible for initiating those responses.

$$\delta\pi_g = \beta\tau P_e \quad (5)$$

where β is a sensitivity parameter, assumed constant. When applied to the general solution (Eqn 3), this leads to yet another solution:

$$g = \chi \frac{(\beta\tau - M)(\psi_s + \pi_c) - \pi_c + \pi_a}{1 + \chi RD_s(\beta\tau - M + \rho)} \quad (6)$$

where a new term, the *guard cell resistive advantage*, $\rho = f_g r_{cg}/R$ ($= R_g/R - 1$), has been introduced for clarity, and π_a is the osmotic pressure in the apoplasm near the stomatal complex. (Eqns 5 & 6 are derived as Eqns A12 & A15 in Appendix 1).

THE MODEL

Equation 6 can be simplified into a compact and useful form that is algebraically similar to the Michaelis–Menten expression for the rate of an enzyme-mediated reaction:

$$g = \frac{g_m(\alpha - \gamma)}{\alpha + K_g} \quad (7)$$

In Eqn 7, g_m is the maximum conductance in the absence of feedback limitation, α is the *guard cell advantage*, K_g is the ‘Michaelis constant’ for α , and γ is the *hydroactive compensation point*. These new terms are defined by Eqns 8–11 and described below:

$$g_m = \frac{\psi_s + \pi_c}{RD_s} \quad (8)$$

$$\alpha \equiv \beta\tau - M + \rho \quad (9)$$

$$K_g = \frac{1}{\chi RD_s} \quad (10)$$

$$\gamma = \frac{\pi_c - \pi_a}{\pi_c + \psi_s} + \rho \quad (11)$$

The maximum conductance, g_m , is the conductance required for transpiration to match the maximum possible flow rate through the plant, which occurs when the gradient that drives water flow to the leaf, $\psi_s - \psi_c$, reaches its most negative possible value, $\psi_s + \pi_c$. Then $g = E/D_s = [(\psi_s + \pi_c)/R]/D_s = g_m$. As g approaches g_m , hydroactive and hydropassive feedback cease to constrain transpiration, so g_m represents the conductance in the absence of feedback limitation.

The guard cell advantage, α , is central to the interpretation of our model. It is the balance of three different effects of leaf water status on stomatal conductance. The first influence, $\beta\tau$, is a positive, *hydroactive* effect that we call the *guard cell metabolic advantage*. The second influence, M , is a negative, *hydromechanical* effect caused by the epidermal mechanical advantage. The third influence, ρ , is a positive hydraulic effect that we call the *guard cell resistive advantage*, caused by any water potential drawdown that may occur from epidermal cells to guard cells.

The ‘Michaelis constant’ for α , K_g , is a measure of the sensitivity of stomatal conductance to ATP; if K_g is small, g saturates at low α , and therefore at lower irradiance. K_g also represents a measure of the intrinsic balance between the hydraulic supply and demand: the transport capacity (hydraulic conductance) of the xylem equals $1/R$, and the evaporative demand of the atmosphere equals D_s . The ‘hydroactive compensation point’, γ , is the value of α required to overcome epidermal turgor to induce stomatal opening. The period of time during which π_g increases in response to light after a period of darkness, but before α reaches γ , is commonly referred to as the *Spannungsphase* (Stålfelt 1929). The resistive advantage (ρ) appears in γ because, if stomata are closed, there is no transpirational flux to create a standing gradient from epidermal to guard cells, so ρ has no effect; in other words, when $\alpha < \gamma$, only $\beta\tau$ is available to overcome M . Our model includes a basal level of ATP (τ_0) that does not depend directly on irradiance, and which makes α positive in the dark, reducing the photon flux density (PFD) required to open stomata. In this context, stomatal opening in darkness would imply $\tau_0 > (\gamma + M - \rho)/\beta$.

Most biologists are familiar with the archetypal topology of Michaelis–Menten curves, so Eqn 7 may help to visualize the model’s behaviour, although the analogy with enzyme kinetics is limited, because g_m and K_m co-vary through R and D_s . For example, an increase in soil water potential raises g_m , permitting higher stomatal conductance and thus greater water use rates. An increase in D_s has two effects: it decreases K_g (the ‘Michaelis constant’ for α), which steepens the response of g to α , making stomata more sensitive to changes in light or photosynthetic capacity, and it decreases g_m , lowering the conductance achieved for a given irradiance and water supply (see Fig. 5a, discussed below).

MODEL BEHAVIOUR

To evaluate the behaviour of the model, we parameterized it using gas exchange and pressure probe experiments on *Vicia faba* L. (Appendix 4). We then performed additional gas exchange experiments to document stomatal responses to changes in environmental variables (Appendix 5) and simulated those experiments, as well as other ‘thought experiments’, in the model (Appendix 3).

Figure 3 compares measured and modelled responses of stomatal conductance to variations in ambient CO₂ concentration (c_a), incident irradiance (I), leaf-to-air water vapour mole fraction gradient (D) and ambient O₂ concentration (pO_2). Conductance declines with increasing D_s and c_a , and rises with incident irradiance (I) (Fig. 3a–c). However, the relative decline with c_a is steeper at low irradiance (Fig. 3a), because ATP concentration responds more steeply to increasing CO₂ supply when photosynthesis is limited by RuBP regeneration (see Fig. 4a, discussed below). Similarly, the light response saturates more quickly at low c_a than at high c_a (Fig. 3b), because photosynthesis is saturated at lower irradiances when c_a is low. Figure 3a also shows another response of g to c_a at high PFD, using a

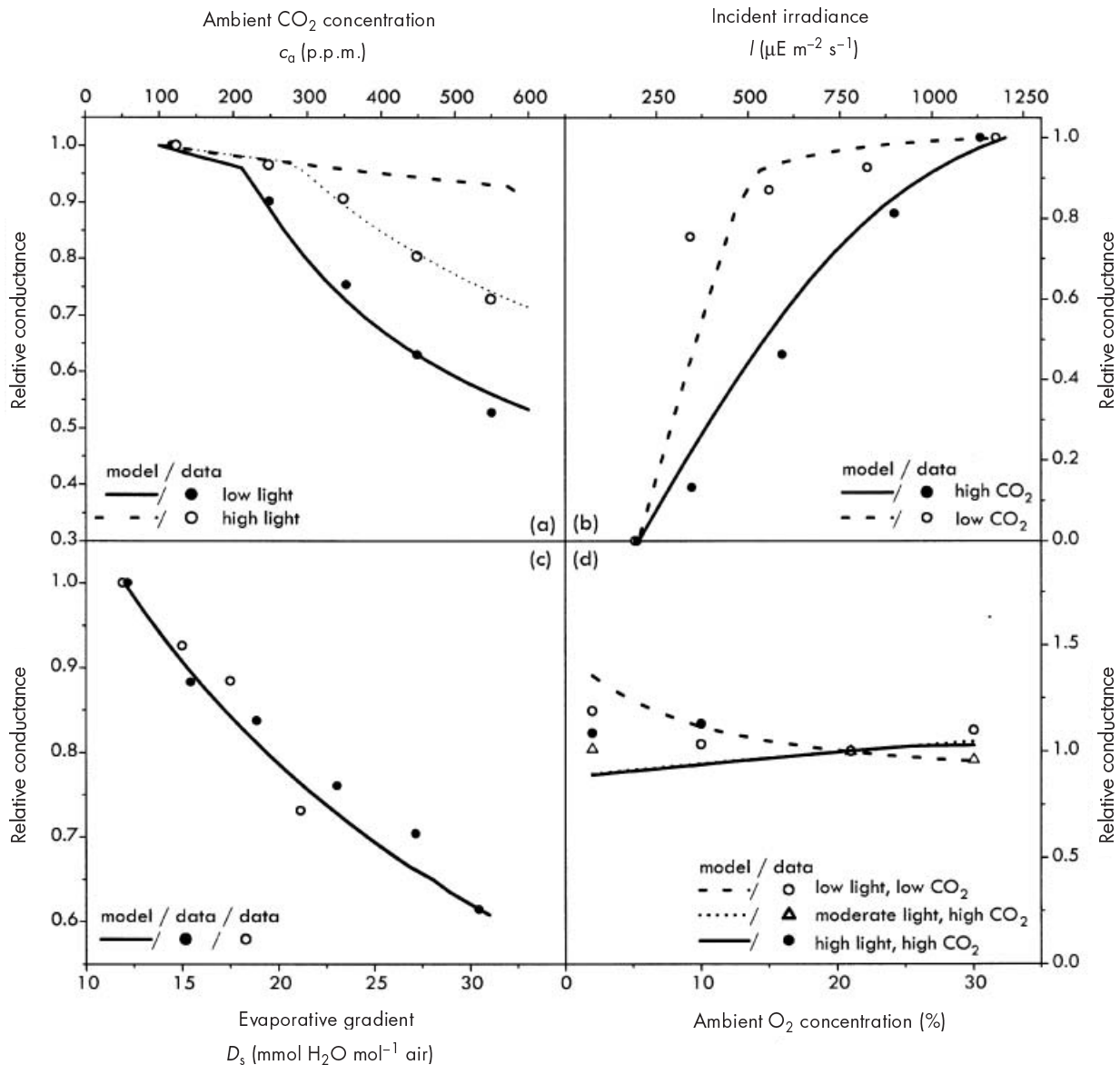


Figure 3. Modelled and measured relationships between relativized g and (a) c_a ; (b) I ; (c) D_s ; and (d) oxygen concentration. g is expressed relative to its value(s) at (a) $c_a = 120$ p.p.m.; (b) both $I = 200$ and $1133 \mu\text{E m}^{-2} \text{s}^{-1}$; (c) $D_s = 10 \text{ mmol mol}^{-1}$; or (d) 21% oxygen. All simulations used the same values for environmental variables as recorded in the gas exchange experiments (methods are described in Appendix 5). Most simulations used the standard parameter values estimated for *Vicia faba* (Table 1), except for the simulation in (a) shown with a thin dotted line, which used a V_m of $185 \mu\text{mol m}^{-2} \text{s}^{-1}$ to demonstrate that the CO_2 response at high light would not appear as 'flat' if V_m were higher.

larger value of V_m (RuBP carboxylation capacity), chosen to make the modelled and observed responses match and to show that the value of c_a at which the response slope changes is strongly dependent on V_m . The value of V_m could not be measured for the leaves whose responses are shown in Fig. 3, so the simulations used a 'standard' value of V_m , calculated as an average from five leaves (see Appendix 4 and Table 1); those five estimates varied by nearly 200%, so it is likely that the measured leaves shown in Fig. 3 each had a different V_m , which may have differed substantially from the 'standard' model value.

The model predicts that stomata can either open or close slightly in response to variations in ambient oxygen concentration, pO_2 and observations showed negligible responses (Fig. 3d). Although the match between our model and the data was less convincing for oxygen than for the CO_2 , light and humidity responses, other stomatal models generally perform worse and they do not predict that the response can be either positive or negative (see Fig. 7, discussed below).

The biochemical substructure of the model, which controls the responses to CO_2 , irradiance, and oxygen, is deeply

embedded in τ (Eqn 6) or α (Eqn 7). In turn, τ and α respond to those environmental factors indirectly, via their effects on photosynthesis as described by the model of Farquhar *et al.* (1980) (Appendix 2). Because we used the τ model of Farquhar & Wong (1984), our model responds to photosynthetic effectors in similar fashion to theirs. However, our model also explicitly includes hydraulic feedback, which warps the responses of g relative to the purely biochemical responses of τ specified by the Farquhar and Wong model. Figure 4 illustrates the linked biochemical and hydraulic control of stomatal conductance by showing how τ , α and g vary with c_i at a series of irradiances. τ , α and g respond to c_i with very similar shapes, although the shape of g versus c_i is slightly different for different values of D_s (Fig. 4b). These features can be understood in terms of the Michaelis–Menten analogy (Eqn 6): near-linearity between g and α implies that K_g is large relative to α . However, K_g and g_m both depend on D_s (Eqn 8). Figure 5a shows that as D_s increases, g saturates more quickly and at a lower value of α , because both K_m and g_m decrease. (Fig. 5c shows how

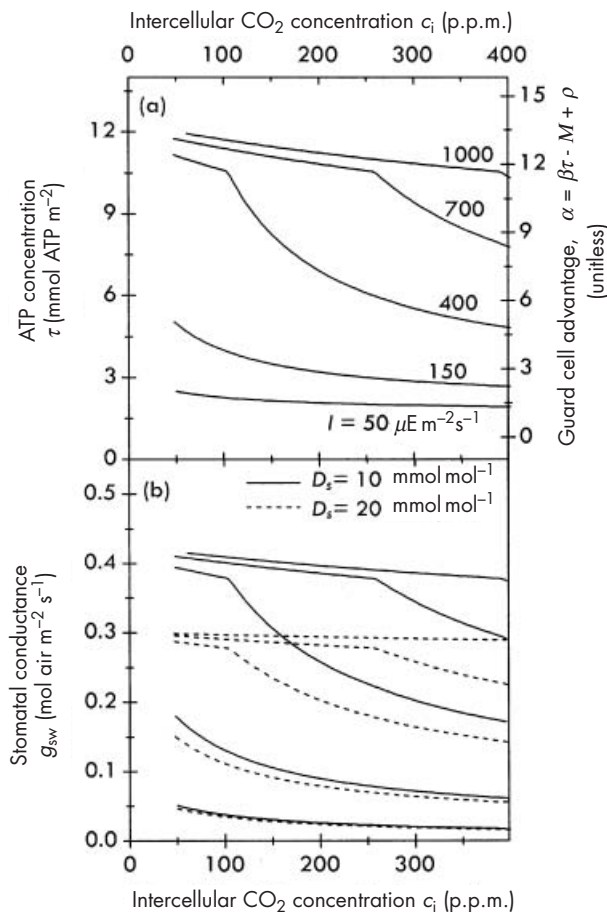


Figure 4. Modelled relationships between intercellular CO₂ concentration (c_i) and (a) ATP concentration (τ , left axis), guard cell advantage (α , right axis) and (b) stomatal conductance, g , at $D_s = 10 \text{ mmol mol}^{-1}$ (solid lines) or 20 mmol mol^{-1} (dashed lines), for a series of different irradiances [as labelled on the curves in panel (a)]. Simulations used standard parameter values (Table 1).

D_s affects the response of g to irradiance itself, rather than α .)

The Michaelis–Menten analogy also provides a way to interpret the effects of declining soil water potential and osmoregulation. If ψ_s declines but epidermal osmotic pressure is ‘osmoregulated’ to match the decline in ψ_s , then g_m will not change, but the hydroactive compensation point, γ , will increase. As a result, the shape of g versus α will be unaffected, but the curve will shift to lower g (Fig. 5b). If, on the other hand, epidermal osmoregulation only matches part of the decline in ψ_s , then g_m will decline and γ will increase further still, changing both the shape and vertical position of the curve. Figure 5d shows how these hypothetical variations in ψ_s and π_c affect the light-response curve itself; note that a higher irradiance is required to open stomata at low ψ_s , because of the larger hydroactive compensation point.

Parameter sensitivity and spatial averaging

Figure 6 shows how parameter variation affects modelled responses to humidity, CO₂ and light. Halving or doubling the residual mechanical advantage (M) has a fairly small effect on the shape and position of most of these responses (Fig. 6a–c); most significantly, the irradiance required to open stomata is higher when M is larger (Fig. 6c), because M decreases the guard cell advantage, requiring higher τ to overcome epidermal turgor and drive α over γ . The insensitivity to M seems paradoxical in light of the importance of the epidermal mechanical advantage to stomatal hydraulics, but the reason is simply that $\beta\tau$, which was introduced for the explicit purpose of overcoming M , is much larger than M . Because R and D_s are algebraically interchangeable in our model (see Eqns 6–10), varying R merely compresses the x -axis for the response to D_s , and has the same effect as variation in D_s on the light-response curve, discussed above (cf. Figs 6f & 5c). Increasing β steepens and magnifies the stomatal responses to each of D_s , c_a and I (Fig. 6g–i), highlighting the dual roles of β as an independent control on stomatal sensitivity and as a link between hydraulic and biochemical factors.

To provide a broader perspective on the model’s behaviour under different parameter regimes, we performed a Monte Carlo analysis, in which many parameters are simultaneously and randomly varied (Fig. 6j–o; see Appendix 3 for details). In Fig. 6j–l, and ten g response curves are shown for D_s , c_a and I ; each curve represents a different leaf (or patch of leaf) with a different set of parameters. Figure 6m–o show the mean and standard deviations among 150 response curves from a set of Monte Carlo simulations. One possible interpretation of the mean curves (solid lines in Fig. 6m–o) is that they represent the behaviour of the model averaged over many ‘leaves’ with different parameter values but identical environmental conditions; however, that interpretation bears the caveat that the averaged ‘leaves’ are functionally independent. The averaging tends to smooth out the kinks caused by transition from Rubisco to light limitation.

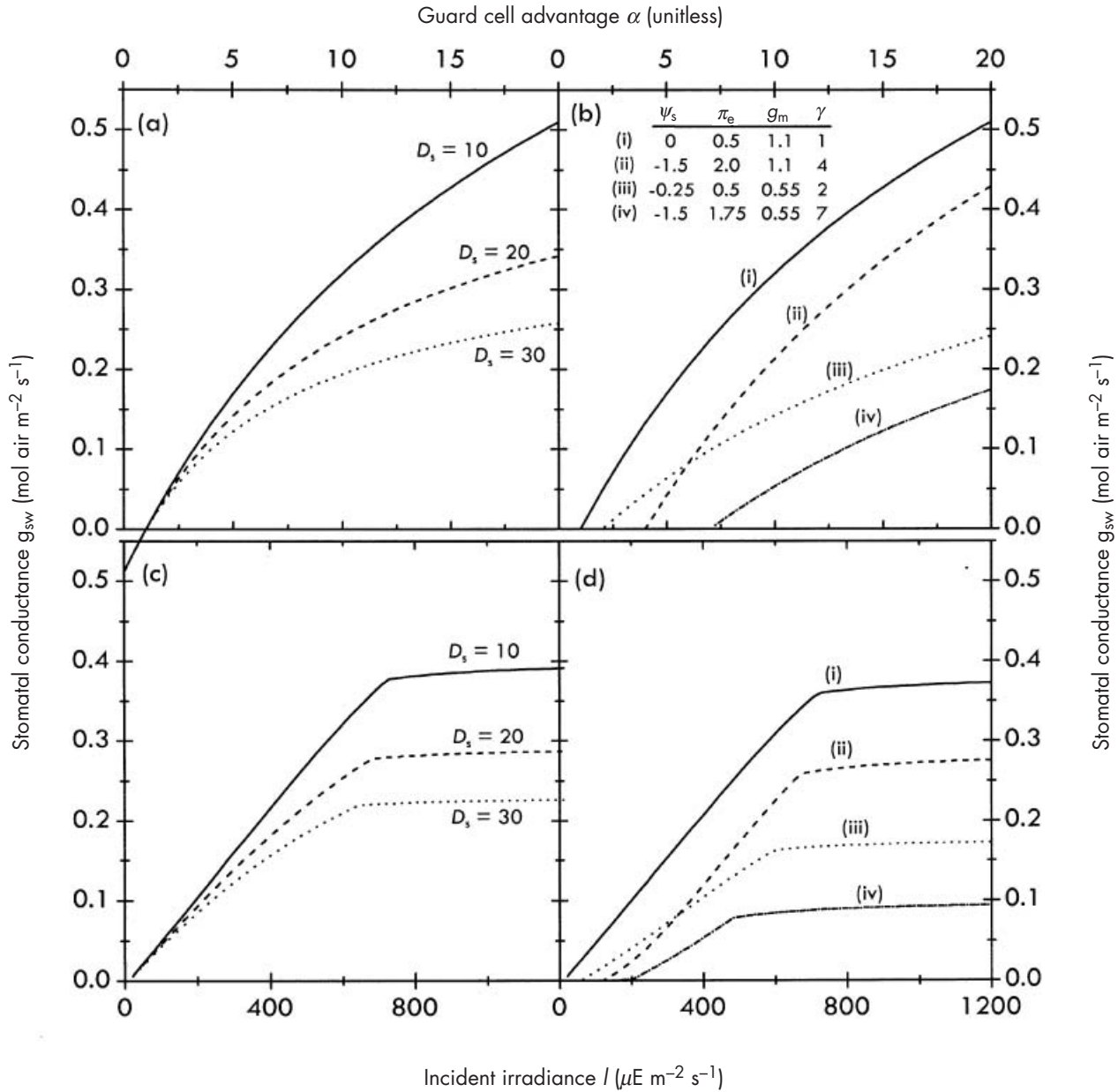


Figure 5. Modelled relationships between stomatal conductance, g and the guard cell advantage, α , at three different evaporative gradients, D_s (a) and three different sets of values for soil water potential, ψ_s and epidermal osmotic pressure, π_e (b). The dashed line in (b) represents a leaf that matches a large decline in ψ_s by an equal and opposite increase in π_e , so that the maximum supply gradient ($\psi_s + \pi_e$) does not change; the dotted line is where ψ_s declines only slightly, but with no osmoregulation; and the dash/dot line is a leaf in which π_e only rises half as much as ψ_s declines, so that g_m drops by half. The hydroactive compensation point (γ , Eqn 11) increases at low ψ_s . The effects of these variations in D_s , ψ_s and π_e on the response of g to incident irradiance, I , are shown in (c) and (d). (Unless stated otherwise, all parameters were set at the 'standard' values given in Table 1).

DISCUSSION

Several stomatal models already exist that can predict most commonly observed variations in stomatal conductance (Jarvis 1976; Ball *et al.* 1987; Leuning 1995; Jarvis & Davies 1998; Dewar 2002; Gao *et al.* 2002; Gutschick & Simonneau 2002; Tuzet *et al.* 2003). However, we are unaware of any other *single* model that is consistent, in both structure and

behaviour, with all of the following empirical constraints: (1) g can vary with E despite constant D_s , and with c_i despite constant c_a ; (2) under most conditions, stomata are fairly unresponsive to oxygen; (3) increases in D_s and R cause conductance to increase transiently, and then decline in the steady state; (4) aperture is more sensitive to epidermal turgor than guard cell turgor, implying that a uniform decrease in turgor should cause stomata to open, rather

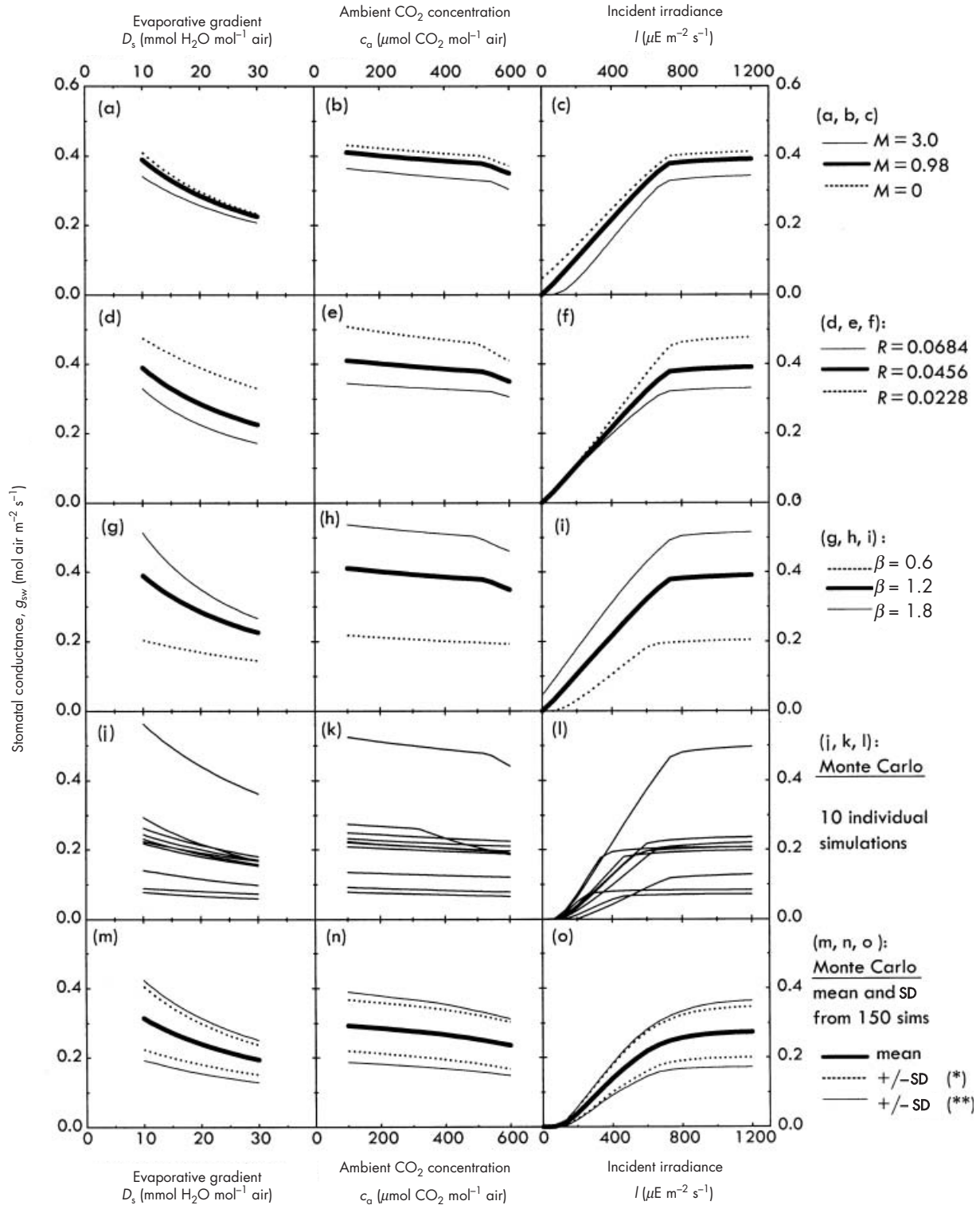


Figure 6. Effects of parameter variation on stomatal responses to D_s , c_a and I predicted by the model. In each of plots (a–i), only one parameter differed from the standard values in Table 1 (M varied in a, b and c; R in d, e and f; and β in g, h and i). Dashed and dotted lines are simulations at non-standard values of M , R or β and solid lines are simulations at standard values (as described in the legends at right). Plots (j–o) show Monte Carlo simulations (detailed in Appendix 3), in which all parameters were randomly varied. (j) (k) (l): ten individual ‘leaves’ with randomly varied parameters. (m) (n) (o): mean \pm standard deviation (SD) among 150 Monte Carlo simulations in which only β , V_m , J_m/V_m , θ and F were varied, using measured values of SD given in Table 1 (*, dashed lines), or in which R , M , χ and π_c were also varied, with $SD = 0.175 \times \text{mean}$ (**, dotted lines).

than close; and (5) increases in ψ_s by root de-pressurization cause immediate, reversible responses that are similar to the responses to D_s and R , suggesting root signals are probably not involved. Our model satisfies each of these constraints:

- 1 *Responses to E and c_i .* It is clear from experimental evidence that the stomatal response to D_s is actually a response to E (Mott & Parkhurst 1991), and that the stomata respond to c_i independently of c_a (Mott 1988). These mechanistic aspects of stomatal behaviour were missing from most early models of stomatal conductance, but several recent models accommodate them (Dewar 2002; Gao *et al.* 2002; Tuzet *et al.* 2003).
- 2 *Oxygen response.* Stomata are generally unresponsive to experimental variation in ambient oxygen partial pressure, pO_2 (Gauhl 1976; Nobel, Longstreth & Hartssock 1978; Farquhar & Wong 1984; Fig. 3d). In our model, stomata respond to changes in pO_2 via changes in guard cell ATP concentration, τ , which we simulated using the model of Farquhar & Wong (1984). That model predicts very small responses to pO_2 (which our hydromechanical framework dampens slightly by its hyperbolic dependence on τ), and negligible responses were measured by gas exchange (Fig. 3d). In contrast, most of the models listed above either do not respond to oxygen at all (Gao *et al.* 2002), or they always respond strongly and negatively (Fig. 7), either by a direct response to net CO_2 assimilation rate (A) (BBL, Gutschick & Simonneau 2002), the ratio of A to $c_i - \Gamma$ (Tuzet *et al.* 2003), or the ratio of gross photosynthetic rate to c_i , $(A + R_d)/c_i$ (Dewar 2002). An exception is the model of Jarvis & Davies (1998), which captures responses to light and CO_2 via the quantity $A_m - A$ (where A_m is photosynthetic capacity). Because A responds negatively to oxygen and A_m does not

respond at all, that model (discussed below) responds positively to pO_2 .

- 3, 4 *Transient wrong-way responses and the epidermal mechanical advantage.* The steady-state responses to short-term variations in D_s , R and ψ_s are typically preceded by a transient change in g in the opposite direction to the steady-state response (Darwin 1898; Raschke 1970; Farquhar & Cowan 1974; Kappen, Andresen & Losch 1987; Comstock & Mencuccini 1998). Hydropassive responses to increases in D_s are controlled by two feedback loops – negative feedback occurs via P_g , positive feedback occurs via P_e (these are labelled as 1 and 2, respectively, in Fig. 2a), and the positive feedback is stronger because of the epidermal mechanical advantage. However, the total feedback must be negative for g to decrease in the steady state as observed. The Gao model achieves this by excluding the P_e loop entirely; the Dewar model achieves it by assuming that $M = 0$, and that a large drawdown in ψ occurs from epidermal to guard cells (Fig. 2b).

Evidence suggests $M > 0$ (DeMichele & Sharpe 1973; Franks *et al.* 1998), and our model takes this evidence at face value. As a result, its net hydropassive feedback is positive (Fig. 2c) and the hydropassive responses to D_s , R and ψ_s are in the ‘wrong’ direction. However, our core hypothesis – that P_e affects the sensitivity of $\delta\pi_g$ to τ (Eqn 5) – creates another negative feedback loop (loop no. 3 in Fig. 2a). This negative *hydroactive* feedback overcomes the hydropassive effects to produce steady-state behaviour consistent with observations. Because changes in $\delta\pi_g$ follow causally from changes in P_e , the latter must be the first to change, so hydropassive ‘wrong-way’ responses must precede hydroactive steady-state responses. The duration of the wrong-way response is determined by the ratio of the time con-

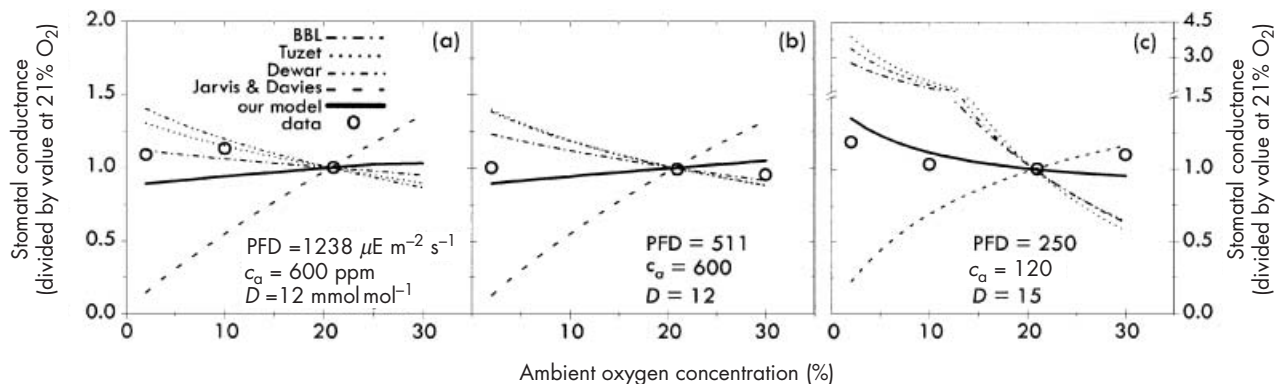


Figure 7. Responses of stomatal conductance to ambient oxygen concentration measured by gas exchange (symbols) and simulated (lines) using five different stomatal models, including the model described in this paper, for three different sets of conditions (a) (b) and (c). g is expressed relative to its value at 21% oxygen in all cases; in (c), the y-axis is broken at $g = 1.5 \text{ mol m}^{-2} \text{ s}^{-1}$ and condensed at higher values to accommodate the large negative responses of some models. Simulations were performed using measured values of A , c_i , c_a , I and pO_2 and the photosynthetic compensation point, Γ , was calculated from the biochemical model of photosynthesis (Appendix 2) (accounting for the dependence of Γ on pO_2). The models of Jarvis & Davies (1998) and Tuzet *et al.* (2003) contain unknown hydraulic parameters, so we only simulated their biochemical components ($A_m - A$ and $A/(c_i - \Gamma)$, respectively; $A_m = J/4$ at the current irradiance), which do not account for hydraulic feedback. (The data and the simulations from our model are the same as in Fig. 3d).

starts for hydraulic equilibration of P_e (following a hydraulic perturbation) and for biochemical adjustment of $\delta\pi_g$ (following a change in P_e) (Farquhar 1973).

By requiring that hydropassive feedback alone produces steady-state hydraulic responses to D_s , the Gao and Dewar models preclude 'wrong-way' responses (Fig. 2d & e). Furthermore, by focusing hydropassive feedback in the ψ gradient from epidermal to guard cells, the Dewar resolution also precludes direct hydropassive effects of either R or ψ_s , thus demanding a separate model to explain those responses (Fig. 2e; Dewar 2002). Our model, in contrast, explains the observed wrong-way and steady-state responses to each of D_s , R and ψ_s in terms of two fast hydraulic feedback loops and one slow biochemical loop that is explicitly linked to the biochemistry of photosynthesis (by way of the putative link between τ and ATP concentration in photosynthesizing cells).

5 Root pressurization and soil drought. Short-term decreases in source water potential (ψ_s) by root de-pressurization have the same effect as increases in D_s and R : conductance increases and then declines in the steady state, and the steady-state response is reversible on short time scales of several hours to a day (Comstock & Menuccini 1998). Our model is based explicitly on the hydropassive influences of D_s , R and ψ_s , and it predicts similar hydropassive responses to each, including root pressurization. Only one of the models listed above (Gao *et al.* 2002) predicts a short-term response to ψ_s without a separate hydraulic model.

Although the weight of empirical evidence suggests that short-term stomatal responses to variations in root pressure are mediated at the leaf level (Schulze & Koppers 1979; Buckley & Mott 2000, 2002b; Sperry 2000), it is also known that [ABA] varies with ψ_s on longer time scales (i.e. several days or more), and ABA probably plays a role in stomatal responses to soil drought. The model of Dewar (2002) and the modification of BBL by Gutschick & Simonneau (2002) also include metabolic responses to changes in transpiration-stream ABA concentration. Our model does not explicitly include a response to chemical signals generated in drying roots; however, the knowledge that ABA stimulates solute efflux from guard cells (Raschke 1987) can be applied to our core hypothesis (Eqn 5) to suggest an avenue for incorporating ABA effects in our model. Suppose active ionic uptake occurs at a rate $\xi\tau$ and passive efflux at a rate $\zeta\delta\pi_g/P_e$ (with ξ and ζ positive coefficients, and $\beta = \xi/\zeta$), so the conductivity of guard cells to ionic efflux is ζ/P_e ; this suggests that ζ should be proportional, and thus β inversely proportional, to ABA concentration: for example, $\beta = \beta_0/[ABA]$. The model of Dewar (2002) contains a similar hypothesis: the rate of outward solute diffusion (d in his paper) depends on xylem sap ABA concentration and epidermal water potential: $d = d_{\min} e^Y$, where $Y = c_1[ABA]\exp(-c_2\psi_e)$ and c_1 and c_2 are positive constants.

Comparison with the Jarvis and Davies model

Among the stomatal models published previously, that of Jarvis & Davies (1998) is most similar to ours. Their model, hereafter referred to as JD, is

$$g = \frac{G(A_m - A)}{1 + sD_s(A_m - A)} \quad (12)$$

where A is the net CO_2 assimilation rate, A_m is the value of A at saturating c_i and s and G are empirical parameters. Jarvis and Davies obtained Eqn 12 by positing abstractly that g is controlled by two linked feedback loops. First, g is proportional to the 'residual photosynthetic capacity', $A_m - A$: that is $g = G^*(A_m - A)$. In the hydromechanical context, this is feedback loop no. 4 in Fig. 2a. Second, the proportionality factor G^* declines from a maximum value, G , with increasing transpiration rate: $G^* = G - sE$. This corresponds to feedback loop no. 3 in Fig. 2a. Comparison of Eqn 12 with Eqns 6–11 suggests $s \propto R$, $G \propto (\psi_s + \pi_e)$ and $(A_m - A) \propto \alpha$. The relations are not precise because two other independent parameters (χ and β) link the relevant features dimensionally in our model, and also because, in describing explicitly the hydraulic feedback loop posited by JD, our model introduces hydromechanical terms such as M , ρ and γ .

Despite these distinctions, both models produce the three photosynthetically related features of stomatal behaviour (the responses to CO_2 and irradiance, and the correlation with photosynthetic capacity) by supposing that stomata respond positively to some measure of *how much faster CO_2 could be fixed if stomata did not limit its supply* (τ in our model, $A_m - A$ in JD). In contrast, other models predict positive responses to I and A_m by including a direct response to A itself; therefore, to predict the negative response to c_i , they must also include an explicitly negative response to some surrogate for CO_2 supply (e.g. c_a , c_i , $c_a - \Gamma$, or $c_i - \Gamma$). The fact that JD predicts a positive response to oxygen in all conditions, whereas the observed response is negative in some conditions and positive in others (see Figs 3d & 7), suggests that if stomata do respond to residual photosynthetic capacity, that response is mediated by a less direct surrogate than $A_m - A$. Guard cell ATP concentration is one obvious candidate for that surrogate.

Co-variation of conductance and photosynthesis

The rationale for modelling g in proportion to A (as most other models do), rather than $A_m - A$ or τ , is based on the observation that g and A co-vary linearly as irradiance varies for a single leaf, or as photosynthetic capacity varies among leaves (Wong, Cowan & Farquhar 1979). Figure 8 illustrates how this feature emerges in our model on a short time scale, as irradiance varies. For any given value of c_i , there are two independent constraints on g that must be satisfied simultaneously: the biochemical and hydromechanical model (Eqn 6 or 7) and the expression for CO_2 diffusion (Eqn A25). The actual state of the leaf corre-

sponds to the intersection of these constraints. Figure 8a shows how these two constraints vary with A (the latter determined by the biochemical model of photosynthesis, and driven by independent variation of c_i) at five different irradiances. The intersection points at different irradiances are almost linearly related. Furthermore, if the same constraints are plotted against c_i rather than A , the intersections occur at similar values of c_i , except at low PFD (Fig. 8b) – showing how our model produces the well-known conservation of c_i , or the ratio of c_i/c_a (Fig. 8c).

The conservation of c_i can also be interpreted mathematically; specifically, the ratio of A/g must be constant. Comparing Eqns A18–A20 at constant c_i with Eqn 7, this implies

$$\frac{\alpha(I) - \gamma}{\alpha(I) + K_g} \propto \begin{cases} J(I) \text{ if } W_e > W_j \\ V_m & \text{else} \end{cases} \quad (13)$$

where the guard cell advantage, α , and potential electron transport rate, J , are expressed as functions of irradiance, I . The two conditions on the right apply when electron transport or Rubisco, respectively, limit photosynthesis. The electron transport-limited condition – that J should increase in similar hyperbolic fashion as α with irradiance – seems reasonable at first glance, because J is calculated from a hyperbolic function of I (Eqn A21). The Rubisco-limited condition, that the hyperbolic function of α on the left should be constant as irradiance increases, implies either that α is insensitive to irradiance or that α is large relative to K_g ; the former reason is stronger here because Fig. 4a verifies that α is relatively insensitive to I under Rubisco-limited conditions (low c_i and high I), whereas K_g is between 6 and 21 and α is between 10 and 14. In summary, our model conserves c_i because (a) when electron transport is limiting, α increases roughly linearly with I , whereas g and J respond hyperbolically to α and I , respec-

tively; and (b) when Rubisco is limiting, V_m is insensitive to irradiance, and α and g are nearly so.

On a longer time scale, our model would produce a correlation between conductance and photosynthetic capacity if all elements of the latter were assumed to scale together, at least in guard cell chloroplasts (this includes carboxylation, electron transport, and photophosphorylation capacities and the potential RuBP and ATP pools – V_m , J_m , p , R_p and a_t , respectively). If that were the case, then guard cell ATP concentration would be simply proportional to V_m for a given irradiance (see Eqns A22 & A23). Conservation of the ratio V_m/J_m (Wullschlegel 1993; Gonzales-Real & Baille 2000; Meir *et al.* 2002) provides some evidence that different elements of photosynthetic capacity scale together, but it does not prove that a_t , R_p and p all co-vary with V_m and J_m in a similar fashion. Furthermore, the hypothesized correlation between g and V_m via τ is mediated by the parameter β (Eqn 6), which may be regulated independently of V_m . Nevertheless, by having g depend explicitly on the concentration of specific components of the photosynthetic apparatus, our model provides a testable, mechanistic hypothesis to explain the observed correlation between conductance and photosynthetic capacity, and thus to study how leaves coordinate the constraints on carbon gain caused by multiple limiting resources – water, nitrogen and light.

Interpretation of the hypothesis that $\delta\pi_g = \beta\tau P_e$

The core hypothesis of our model, Eqn 5 (Eqn A12 in Appendix 1) actually consists of two complementary hypotheses. First, the guard cell osmotic gradient must increase with the turgor pressure of adjacent epidermal cells. We suggested an interpretation of this putative response in Appendix 1, following the reasoning of Dewar

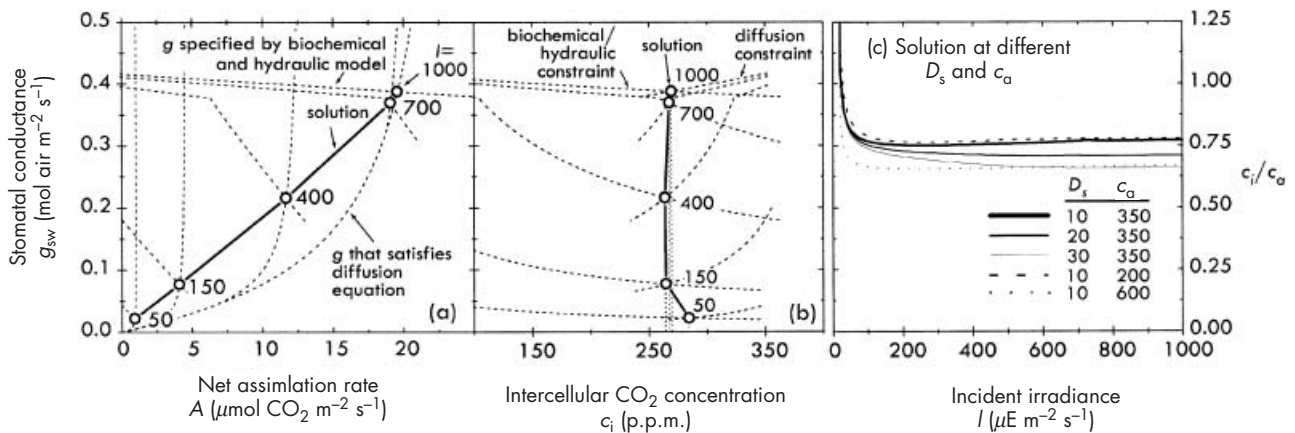


Figure 8. Diagram showing the two independent constraints that link stomatal conductance to net assimilation rate (A) and intercellular CO_2 concentration (c_i). The 'biochemical constraint' on g is Eqn 6 or Eqn 7, in which g_{sw} depends indirectly on c_i via ATP concentration. The 'diffusion' constraint is simply $1.6 A(c_i)/(c_a - c_i)$, where $A(c_i)$ is the biochemical model of photosynthesis given in Appendix 2. Panel (a) shows these constraints as relationships between g and A and panel (b) shows them as relationships between g and c_i itself. At any given irradiance, the actual state of the leaf corresponds to the intersection of the two constraints. In the solution (as opposed to in either constraint alone), g versus A is roughly linear and c_i is nearly constant. Panel (c) shows how the solution, expressed in terms of the ratio of c_i/c_a , varies with irradiance for different values of D_s and c_a .

(2002), wherein the resistance to passive osmotic leakage out of guard cells is proportional to epidermal turgor, but our model does not rest on this interpretation. Second, the guard cell osmotic gradient must be proportional to the cytosolic ATP concentration in guard cells, τ . This hypothesis is supported by recent data of Tominaga *et al.* (2001) showing that guard cell chloroplasts in *Commelina benghalensis* supply the ATP necessary to drive proton pumping, and that the pumping rate is limited by ATP supply.

Observed stomatal responses (e.g. Fig. 3) place empirical constraints on the behaviour of τ : it must increase with light, decrease with CO₂ and be fairly insensitive to oxygen. The model of Farquhar & Wong (1984) behaves in this manner, suggesting that it is an *empirically* adequate submodel for τ . However, for this submodel to be interpreted as a *mechanistic* component of our model, a third core hypothesis must be satisfied: that [ATP] is controlled by similar biochemical processes in guard cells and mesophyll cells. Some evidence is inconsistent with this hypothesis – for example, biochemical assays (Outlaw *et al.* 1979; Outlaw 1989) have reported no evidence for substantial Calvin cycle activity in guard cells – but other evidence supports it. Cardon & Berry (1992) found that guard cell fluorescence in discs from white areas of variegated *Tradescantia albiflora* leaves responded to CO₂ as would be expected if Rubisco-limited CO₂ fixation were the major sink for photosynthetic ATP, and that oxygen produced a response, but only at low CO₂ – also consistent with a role for Rubisco. Those results were recently confirmed by Lawson *et al.* (2002), whose apparatus allowed concurrent measurements of guard and mesophyll cell chloroplast fluorescence in green regions of *T. albiflora* leaves; they also extended the results to a second species (*Commelina communis*).

It is worth noting that our model for stomatal conductance does not rest on the validity of any particular hypothesis about the biochemical pathways responsible for controlling guard cell [ATP]; mathematically, the model rests only on the assertion that guard cells contain some quantity, τ , that responds to changes in environmental conditions in the manner required to produce observed conductance responses. If future experiments suggest τ is not [ATP], then the mechanism underlying the biochemical component of our model must be re-interpreted, but the model's hydromechanical framework – arguably its main novel feature – would be unaffected by such evidence. Our model shows how observed stomatal responses to non-hydraulic environmental factors (such as irradiance and [CO₂]) can be integrated with both 'wrong-way' and steady-state responses to hydraulic factors (such as humidity, xylem resistance and source water potential) under the auspices of a single mechanism of guard cell osmotic regulation.

CONCLUSION

This study presents a mathematical model that predicts stomatal conductance from the balance of opposing hydro-mechanical and biochemical influences in and around guard cells. These influences interact directly in the control

of the guard cell osmotic gradient, which we hypothesize is proportional to the concentration of ATP in guard cells (a sensor of the balance between CO₂ supply and demand in photosynthesis) and to the turgor pressure of adjacent epidermal cells (a sensor of the balance between H₂O supply and demand in transpiration). We used a previously published model based on C₃ mesophyll photosynthesis (Farquhar & Wong 1984) to simulate τ , parameterized and tested the stomatal model directly for *Vicia faba* L. and found that it reproduces the well-known short-term stomatal responses to environmental variables. Unlike other models, ours also predicts that stomata should be relatively insensitive to the ambient oxygen concentration, and it accounts for the epidermal mechanical advantage, which controls critically the direction of passive stomatal responses to hydraulic perturbations.

Our model represents a step towards producing a stomatal model based entirely on reduced processes at the cellular level. As such, it allows properties of gas exchange in intact leaves to be interpreted directly in terms of processes at the cellular level, and it suggests a direct mechanistic nexus between hydraulic and photosynthetic capacities. Finally, our model provides a mathematical framework to help understand how plants coordinate the economic tradeoffs of multiple limiting resources in intact leaves.

ACKNOWLEDGMENTS

We thank Rand Hooper for tireless, patient, and always excellent technical assistance, and three anonymous reviewers for helpful comments that led to substantial improvements in the manuscript. This work was supported by salary to T.N.B. from the Cooperative Research Centre for Greenhouse Accounting at the Australian National University, Canberra.

REFERENCES

- Badger M.R. & Andrews T.J. (1974) Effects of CO₂, O₂ and temperature on a high-affinity form of ribulose disphosphate carboxylase-oxygenase from spinach. *Biochemica et Biophysica Research Communication* **60**, 204–210.
- Ball M.C. & Critchley C. (1982) Photosynthetic responses to irradiance by the grey mangrove, *Avicennia marina*, grown under different light regimes. *Plant Physiology* **70**, 1101–1106.
- Ball J.T., Woodrow I.E. & Berry J.A. (1987) A model predicting stomatal conductance and its contribution to the control of photosynthesis under different environmental conditions. In *Progress in Photosynthesis Research* (ed. J. Biggens), pp. 221–224. Martinus-Nijhoff Publishers, Dordrecht, The Netherlands.
- Buckley T.N. & Mott K.A. (2000) Stomatal responses to non-local changes in PFD: evidence for long-distance hydraulic interactions. *Plant, Cell and Environment* **23**, 301–309.
- Buckley T.N. & Mott K.A. (2002a) Dynamics of stomatal water relations during the humidity response: implications of two hypothetical mechanisms. *Plant, Cell and Environment* **25**, 407–419.
- Buckley T.N. & Mott K.A. (2002b) Stomatal water relations and the control of hydraulic supply and demand. *Progress in Botany* **63**, 309–325.

- Caemmerer S.V., Evans J.R., Hudson G.S. & Andrews T.J. (1994) The kinetics of ribulose-1,5-bisphosphate carboxylase/oxygenase in vivo inferred from measurements of photosynthesis in leaves of transgenic tobacco. *Planta* **195**, 88–97.
- Cardon Z.G. & Berry J.A. (1992) Effects of O₂ and CO₂ concentration in the steady-state fluorescence yield of single guard cell pairs in intact leaf discs of *Tradescantia albiflora*. *Plant Physiology* **99**, 1238–1244.
- Comstock J.P. & Mencuccini M. (1998) Control of stomatal conductance by leaf water potential in *Hymenoclea salsola* (T. & G.), a desert shrub. *Plant, Cell and Environment* **21**, 1029–1038.
- Darwin F. (1898) Observations on stomata. *Philosophical Transactions of the Royal Society of London, Series B* **190**, 531–621.
- DeMichele D.W. & Sharpe P.J.H. (1973) An analysis of the mechanics of guard cell motion. *Journal of Theoretical Biology* **41**, 77–96.
- Dewar R.C. (1995) Interpretation of an empirical model for stomatal conductance in terms of guard cell function. *Plant, Cell and Environment* **18**, 365–372.
- Dewar R.C. (2002) The Ball–Berry–Leuning and Tardieu–Davies stomatal models: synthesis and extension within a spatially aggregated picture of guard cell function. *Plant, Cell and Environment* **25**, 1383–1398.
- Edwards M., Meidner H. & Sheriff D.W. (1976) Direct measurements of turgor pressure potentials of guard cells. II. The mechanical advantage of subsidiary cells, the Spannungsphase, and the optimum leaf water deficit. *Journal of Experimental Botany* **96**, 163–171.
- Farquhar G.D. (1973) A Study of the Response of Stomata to Perturbations of Environment. PhD Thesis. Australian National University, Canberra, Australia.
- Farquhar G.D. & Cowan I.R. (1974) Oscillations in stomatal conductance. The influence of environmental gain. *Plant Physiology* **54**, 769–772.
- Farquhar G.D. & Wong S.C. (1984) An empirical model of stomatal conductance. *Australian Journal of Plant Physiology* **11**, 191–210.
- Farquhar G.D., Caemmerer S.V. & Berry J.A. (1980) A biochemical model of photosynthetic CO₂ assimilation in leaves of C₃ species. *Planta* **149**, 78–90.
- Fischer R.A. & Hsiao T.C. (1968) Stomatal opening in isolated epidermal strips of *Vicia faba*. II. Responses to KCl concentration and the role of potassium absorption. *Plant Physiology* **43**, 1953–1958.
- Franks P.J., Cowan I.R. & Farquhar G.D. (1998) A study of stomatal mechanics using the cell pressure probe. *Plant, Cell and Environment* **21**, 94–100.
- Franks P.J., Cowan I.R., Tyerman S.D., Cleary A.L., Lloyd J. & Farquhar G.D. (1995) Guard cell pressure/aperture characteristics measured with the pressure probe. *Plant, Cell and Environment* **18**, 795–800.
- Gao Q., Zhao P., Zeng X., Cai X. & Shen W. (2002) A model of stomatal conductance to quantify the relationship between leaf transpiration, microclimate and soil water stress. *Plant, Cell and Environment* **25**, 1373–1381.
- Gauhl E. (1976) Photosynthetic response to varying light intensity in ecotypes of *Solanum dulcamara* L. from shaded and exposed environments. *Oecologia* **22**, 275–286.
- Gonzales-Real M.M. & Bailla A. (2000) Changes in leaf photosynthetic parameters with leaf position and nitrogen content within a rose plant canopy (*Rosa hybrida*). *Plant, Cell and Environment* **23**, 351–363.
- Gutschick V.P. & Simonneau T. (2002) Modelling stomatal conductance of field-grown sunflower under varying soil water content and leaf environment: comparison of three models of stomatal response to leaf environment and coupling with an abscisic acid-based model of stomatal response to soil drying. *Plant, Cell and Environment* **25**, 1423–1434.
- Haefner J.W., Buckley T.N. & Mott K.A. (1997) A spatially explicit model of patchy stomatal responses to humidity. *Plant, Cell and Environment* **20**, 1087–1097.
- Jarvis P.G. (1976) The interpretation of the variations in leaf water potential and stomatal conductance found in canopies in the field. *Philosophical Transactions of the Royal Society of London, Series B* **273**, 593–610.
- Jarvis A.J. & Davies W.J. (1998) The coupled response of stomatal conductance to photosynthesis and transpiration. *Journal of Experimental Botany* **49**, 399–406.
- Kappen L., Andresen G. & Losch R. (1987) In situ observations of stomatal movements. *Journal of Experimental Botany* **38**, 126–141.
- Lawson T., Oxborough K., Morison J.I.L. & Baker N.R. (2002) Responses of photosynthetic electron transport in stomatal guard cells and mesophyll cells in intact leaves to light, CO₂, and humidity. *Plant Physiology* **128**, 52–62.
- Leuning R. (1995) A critical appraisal of a combined stomatal-photosynthesis model for C₃ plants. *Plant, Cell and Environment* **18**, 339–357.
- Meir P., Kruijt B., Broadmeadow M., Barbosa E., Kull O., Carswell F., Nobre A. & Jarvis P.G. (2002) Acclimation of photosynthetic capacity to irradiance in tree canopies in relation to leaf nitrogen concentration and leaf mass per unit area. *Plant, Cell and Environment* **25**, 343–357.
- Monteith J.L. (1995) A reinterpretation of stomatal responses to humidity. *Plant, Cell and Environment* **18**, 357–364.
- Mott K.A. (1988) Do stomata respond to CO₂ concentrations other than intercellular? *Plant Physiology* **86**, 200–203.
- Mott K.A. & Franks P.J. (2001) The role of epidermal turgor in stomatal interactions following a local perturbation in humidity. *Plant, Cell and Environment* **24**, 657–662.
- Mott K.A. & Parkhurst D.F. (1991) Stomatal response to humidity in air and helox. *Plant, Cell and Environment* **14**, 509–515.
- Nobel P.S., Longstreth D.H. & Hartssock T.L. (1978) Effect of water stress on the temperature optima of net CO₂ exchange for two desert species. *Physiologia Plantarum* **44**, 97–101.
- Outlaw W.H.J. (1989) Critical examination of the quantitative evidence for and against photosynthetic CO₂ fixation by guard cells. *Physiologia Plantarum* **77**, 275–281.
- Outlaw W.H.J., Manchester J., Di Camelli C.A., Randell D.D., Rapp B. & Veith G.M. (1979) Photosynthetic carbon reduction pathway is absent in chloroplasts of *Vicia faba* guard cells. *Proceedings of the National Academy of Sciences of the USA* **76**, 6371–6375.
- Press W.H., Teukolsky S.A., Vetterling W.T. & Flannery B.P. (1992) *Numerical Recipes in C++: the Art of Scientific Computing*. Cambridge University Press, Cambridge, UK.
- Raschke K. (1970) Stomatal responses to pressure changes and interruptions in the water supply of detached leaves of *Zea mays* L. *Plant Physiology* **45**, 415–423.
- Raschke K. (1987) Action of abscisic acid on guard cells. In *Stomatal Function* (eds E. Zeiger, G.D. Farquhar & I.R. Cowan), pp. 253–279. Stanford University Press, Stanford, CA, USA.
- Schulze E.D. & Koppers M. (1979) Short-term and long-term effects of plant water deficits on stomatal response to humidity in *Corylus avellana* L. *Planta* **146**, 319–326.
- Shackel K.A. & Brinkmann E. (1985) In situ measurement of epidermal cell turgor, leaf water potential, and gas exchange in *Tradescantia virginiana* L. *Plant Physiology* **78**, 66–70.
- Sharpe P.J.H., Wu H. & Spence R.D. (1987) Stomatal mechanics.

In *Stomatal Function* (eds E. Zeiger, G.D. Farquhar & I.R. Cowan), pp. 91–114. Stanford University Press, Stanford, CA, USA.

- Sperry J.S. (2000) Hydraulic constraints on gas exchange. *Agricultural and Forest Meteorology* **104**, 13–23.
- Stålfelt M.G. (1929) Die Abhängigkeit der Spaltöffnungsreaktionen von der Wasserbilanz. *Planta* **8**, 287–296.
- Tominaga M., Kinoshita T. & Shimazaki K.-i. (2001) Guard-cell chloroplasts provide ATP required for H⁺ pumping in the plasma membrane and stomatal opening. *Plant and Cell Physiology* **42**, 795–802.
- Tuzet A., Perrier A. & Leuning R. (2003) A coupled model of stomatal conductance, photosynthesis, and transpiration. *Plant, Cell and Environment* **26**, 1097–1116.
- Wong S.C., Cowan I.R. & Farquhar G.D. (1979) Stomatal conductance correlates with photosynthetic capacity. *Nature* **282**, 424–426.
- Wullschlegel S.D. (1993) Biochemical limitations to carbon assimilation in C₃ plants – A retrospective analysis of the A/c_i curves from 109 species. *Journal of Experimental Botany* **44**, 907–920.

Received 13 December 2002; accepted for publication 18 March 2003

APPENDIX 1: DERIVATION OF HYDROMECHANICAL MODEL

General hydromechanical model

The hydromechanical core of our model consists of five relationships. First, stomatal conductance (g) is proportional to stomatal aperture (a):

$$g = \frac{\chi}{c} a \quad (\text{A1})$$

where χ and c are proportionality constants. Second, stomatal aperture is a linear combination of guard cell and epidermal turgor pressures (P_g and P_e , respectively):

$$a = c(P_g - \hat{m}P_e) \quad (\text{A2})$$

Formally, P_e represents the turgor pressure of ‘subsidiary’ epidermal cells, that is, the cells that immediately adjoin the guard cells, but as pressure probe experiments (Franks *et al.* 1995, 1998; Mott & Franks 2001) have shown no systematic variation in turgor between subsidiary and non-subsidiary epidermal cells, P_e can also be interpreted as the turgor of the ‘bulk’ epidermis. The parameter \hat{m} in Eqn A2 is sometimes called the ‘mechanical advantage of the epidermis’ and labelled as ‘ m ’. (We use a different symbol in Eqn A2 because m is actually defined as $-(\partial a/\partial P_e)/(\partial a/\partial P_g)$, and because Franks *et al.* (1995, 1998) reported a non-linear relationship between a , P_g and P_e , so $\hat{m} \neq m$ formally. We fitted Eqn A2 to the Franks data (Fig. 9a & b) and found $\hat{m} = 1.98$). Third, P_g and P_e are sums of water potential (ψ) and osmotic pressure (π) terms:

$$P_g = \psi_g + \pi_g, \quad P_e = \psi_e + \pi_e \quad (\text{A3})$$

(where π_g and π_e are positive by convention.) Fourth, each of these water potentials forms one end of a gradient that drives a liquid flow in proportion to the transpiration rate

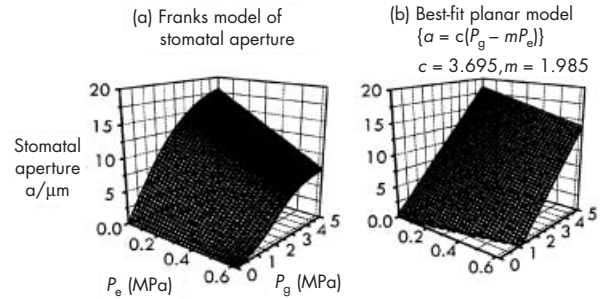


Figure 9. The dependence of stomatal aperture, a , on guard cell turgor pressure, P_g and epidermal cell turgor pressure, P_e . (a) Experimental data of Franks *et al.* (1998), using the parameters for low P_e calculated by Buckley & Mott (2002a). (b) Equation A2 $a = \max[c(P_g - \hat{m}P_e), 0]$ fitted to the Franks data.

(E). To describe these flows, we consider the leaf diagrammed in Fig. 1, in which transpiration occurs from three sites (mesophyll, epidermal and guard cells) in the proportions f_m , f_e and f_g , respectively (note $f_m + f_e + f_g = 1$) and which is fed water by a single conduit with zero capacitance and resistance given by r_{sx} , connected to the soil at water potential ψ_s . Then

$$E = \frac{\psi_s - \psi_x}{r_{sx}} = \frac{\psi_x - \psi_e}{(f_e + f_g)r_{xe}} = \frac{\psi_e - \psi_g}{f_g r_{eg}} \quad (\text{A4})$$

where r_{xe} and r_{eg} are resistances from the xylem to epidermal cells and from epidermal to guard cells, respectively. Equation (A4) can be rewritten in terms of ψ_s and ψ_e , or ψ_s and ψ_g :

$$\psi_e = \psi_s - RE \quad (\text{A5})$$

$$\psi_g = \psi_s - R_g E$$

where $R \equiv r_{sx} + (f_e + f_g)r_{xe}$ and $R_g \equiv R + f_g r_{eg}$. Fifth, transpiration rate is the product of stomatal conductance and the evaporative gradient (D_s , the difference in water vapour mole fraction between the leaf's intercellular spaces and the boundary layer):

$$E = gD_s \quad (\text{A6})$$

To derive Eqn 1 in the main text, we set $\hat{m} = 0$ in Eqn A2 so that $g = \chi P_g$, apply this to Eqn A3 to give $g = \chi[(\psi_s - R_g E) + \pi_g]$ and then apply Eqn A6 and rearrange to solve for g :

$$g = \chi \frac{\psi_s + \pi_g}{1 + \chi R_g D_s} \quad (\text{A7})^\circ$$

This expression is marked with a $^\circ$ symbol to indicate that it is not part of our model; it is a special case derived for heuristic purposes. To derive Eqn 3 in the main text, we combine Eqns A1–A3 and A5 directly to yield

$$g = \chi[(\psi_s - R_g E) + \pi_g] - \hat{m}[(\psi_s - RE) + \pi_e] \quad (\text{A8})$$

Pooling similar terms and defining the *residual mechanical advantage* of the epidermis as $M \equiv (\hat{m} - 1)$, we have:

$$g = \chi[-M(\psi_s + \pi_c) + (\pi_g - \pi_c) + (MR - f_g r_{eg})E] \quad (\text{A9})$$

Finally, using Eqn (A6) to replace E with gD_s and solving for g yields:

$$g = \chi \frac{-M(\psi_s + \pi_c) + \pi_g - \pi_c}{1 - \chi R(M - f_g r_{eg}/R)D_s} \quad (\text{A10})$$

Equation 4 in the main text is found simply by setting $M = 0$ in Eqn A10:

$$g = \chi \frac{\pi_g - \pi_c}{1 + \chi R D_s} \quad (\text{A11})^\circ$$

Again, Eqn A11 is marked with a $^\circ$ symbol to indicate that it is not part of our model.

Steady-state model with metabolic regulation

To derive our steady-state model, we constrain Eqn A10 with an expression for the steady-state guard cell osmotic gradient ($\delta\pi_g = \pi_g - \pi_a$, where π_a is the osmotic pressure of the apoplastic region near the stomatal complex, assumed uniform). We propose two hypotheses. First, $\delta\pi_g$ is proportional to the concentration of ATP in guard cells, represented by the symbol τ . Second, the sensitivity of $\delta\pi_g$ to τ is proportional to epidermal turgor pressure, P_e . These hypotheses imply:

$$\delta\pi_g = \beta\tau P_e \quad (\text{A12})$$

where β is an empirical coefficient. Applying Eqn A12 to Eqn A9, we have

$$g = \chi(-M(\psi_s + \pi_c) + (\beta\tau P_e + \pi_a - \pi_c) + (MR - f_g r_{eg})E) \quad (\text{A13})$$

We use Eqns A3 and A5 to express P_e in terms of ψ_s , π_c , R and E and rearrange to pool similar terms:

$$g = \chi((\beta\tau - M)(\psi_s + \pi_c) - (\pi_c - \pi_a) + (-\beta\tau R + MR - f_g r_{eg})E) \quad (\text{A14})$$

Finally, we apply Eqn A6 and solve for g :

$$g = \chi \frac{(\beta\tau - M)(\psi_s + \pi_c) - \pi_c + \pi_a}{1 + \chi R D_s (\beta\tau - M + \rho)} \quad (\text{A15})$$

This is Eqn 6 in the main text. A new unitless term, ρ , defined as $f_g r_{eg}/R$, has been introduced in Eqn A15. (Note that ρ also equals $(R_g - R)/R$ or $R_g/R - 1$). The *hydroactive* effect represented by $\beta\tau$ overcomes the *hydropassive* effect caused by $-M$ and the occurrence of a transient *hydropassive* response to perturbations in either D_s , R , or ψ_s is easily explained by a finite time constant for adjustment of $\delta\pi_g$ in response to changes in P_e .

The model form given in Eqn A15 is not strictly a closed-form solution because D_s is the evaporative gradient from the intercellular spaces to the leaf surface and it can not be measured directly. It is inferred from the leaf-to-ambient-air gradient, D , given the ratio of stomatal conductance, g , and boundary layer resistance, r_{bw} ; thus, D_s is an implicit function of g . The correct closed form solution is the greater

root of a quadratic expression: $g = [-q_1 + (q_1^2 - 4q_2q_0)^{0.5}]/2q_2$, where the quadratic coefficients q_n are given by Eqn A16:

$$\begin{aligned} q_2 &= r_{bw} \\ q_1 &= 1 + \chi[RD\alpha - r_{bw}(\psi_s + \pi_c)(\alpha - \gamma)] \\ q_0 &= -\chi(\psi_s + \pi_c)(\alpha - \gamma) \end{aligned} \quad (\text{A16})$$

The terms α and γ are defined by Eqns 9 and 11 in the main text. Equation A15 is easily obtained by substituting $r_{bw} = 0$ and $D_s = D$ into the above.

The meaning of β

Following Dewar (2002), one possible interpretation of the metabolic response parameter, β (Eqn A12) is that the rate of active solute uptake by guard cells (π^+) is proportional to τ ($\pi^+ = \xi\tau$) and that the *resistance* to outward diffusion is proportional to P_e , so that the rate of passive efflux is $\pi^- = \zeta\delta\pi_g/P_e$. The net rate of change of π_g , $\pi^+ - \pi^-$, is zero at steady state, so that

$$\xi\tau = \zeta\delta\pi_g/P_e \Rightarrow \delta\pi_g = \frac{\xi}{\zeta}\tau P_e \quad (\text{A17})$$

In this interpretation, ζ is the passive efflux rate at a reference P_e of 1 MPa, and ξ is the pumping rate per mmol m^{-2} of ATP. This interpretation would appear to be challenged by experimental data of Fischer & Hsiao (1968) showing that stomata in epidermal peels with punctured epidermal cells remain open after being first illuminated, then placed in darkness. However, the possibility remains that the conductance of guard cell membranes to outward solute diffusion is normally near zero, and that intact epidermal cells are required to generate a signal that causes them to leak (in the absence of closing signals arising in distant tissues, such as ABA from drying roots).

APPENDIX 2: DESCRIPTION OF THE MODEL OF [ATP]

Farquhar & Wong (1984) derived expressions for the concentration of ATP in mesophyll chloroplasts of leaves of C_3 species, from the mathematical model of photosynthesis presented by Farquhar *et al.* (1980). The latter model is

$$A = \left(1 - \frac{\Gamma^*}{p_i}\right) \cdot \min\{W_c, W_j\} - R_d \quad (\text{A18})$$

where A is the leaf net CO_2 assimilation rate, Γ^* is the photorespiratory compensation point, p_i is the partial pressure of CO_2 in the intercellular spaces, W_c is the RuBP-saturated rate of RuBP carboxylation, W_j is the rate of carboxylation that can be sustained by the current rate of electron transport, and R_d is the rate of leaf respiration that continues in the dark. W_c and W_j are given by

$$W_c = \frac{V_m p_i}{p_i + K_c(1 + p\text{O}_2/K_o)} \quad (\text{A19})$$

$$W_j = \frac{Jp_i}{4(p_i + 2\Gamma^*)} \quad (\text{A20})$$

where K_c and K_o are the Rubisco Michaelis–Menten constants for RuBP carboxylation and oxygenation, respectively, V_m is the maximum velocity of RuBP carboxylation, J is the potential electron transport rate and pO_2 is the partial pressure of oxygen in the intercellular spaces. (Γ^* depends on pO_2 by the empirical relation: $\Gamma^* = k_o K_c pO_2 / (2k_c K_o)$, where k_o and k_c are the turnover numbers for Rubisco oxygenation and carboxylation, respectively, by Rubisco; we assumed that $k_o/2k_c = 0.105$, as found at 25 °C by Badger & Andrews 1974). Following Farquhar & Wong (1984), J is modelled as the hyperbolic minimum of the light-saturated potential electron transport rate (J_m) and the product of incident irradiance (I) with the parameter F (F is the product of leaf absorptivity to PAR and the effective quantum yield), so that

$$J = \min\{J_m, FI, \theta_j\} \quad (\text{A21})$$

where $\min\{x, y, \theta\}$ is the root Z of a quadratic expression given by $\theta Z^2 - (x + y)Z + xy = 0$. The concentration of ATP provided by photophosphorylation is modelled as one of two different values: τ_c , which applies when $W_c < W_j$, and τ_j , which applies when $W_j < W_c$:

$$\tau_c = a_t - p \frac{W_c}{W_j} \quad (\text{A22})$$

$$\tau_j = (a_t - p) \left(\frac{V_r}{V_m} - 1 \right) / \left(\left[\frac{W_c}{W_j} \right] \frac{V_r}{V_m} - 1 \right) \quad (\text{A23})$$

$$\tau \equiv \tau_0 + \begin{cases} \tau_c & \text{if } W_c < W_j \\ \tau_j & \text{else} \end{cases} \quad (\text{A24})$$

In Eqn A24, τ_0 is the basal level of ATP provided by *other* processes, such as ongoing mitochondrial respiration. a_t is the total concentration of adenylates ($\tau + [\text{ADP}]$), p is the concentration of photophosphorylation sites and V_r is the CO_2 - and Rubisco-saturated potential rate of carboxylation (i.e. limited only by the availability of CO_2 acceptors). V_r and V_m are given by $k_c R_p$ and $k_c E_t$, respectively, where k_c is the Rubisco turnover number for RuBP carboxylation, R_p is the potential RuBP pool size and E_t is the concentration of Rubisco active sites (proportional to V_m). The simulations presented here assumed that a_t , p , J_m and R_p are proportional to E_t , and therefore to V_m , on the premise that all components of the photosynthetic apparatus should scale with one another to maintain a functional balance. Therefore, in practice, V_r , a_t and p were each calculated as fixed proportions of V_m , given in Table 1. The numerical value of τ_0 was chosen arbitrarily, to satisfy the empirical constraints that c_i increases as irradiance approaches zero (e.g. Ball & Critchley 1982) (which requires that A decline to zero at a higher irradiance than g , that is, $\alpha > \gamma$ at the photosynthetic light compensation point), and that stomata close in the dark (i.e. $\alpha < \gamma$ at zero irradiance). Note that τ does not *numerically* represent guard cell ATP concentra-

tion *per se*; rather, we assume the latter is proportional to τ , and use parameter values that are based on mesophyll pools and expressed on a leaf area basis.

APPENDIX 3: NUMERICAL PROCEDURES

A value for τ is needed to solve the expression for stomatal conductance (Eqn A15), but this in turn requires a value for c_i , which depends on stomatal conductance according to the standard expression for CO_2 diffusion through stomata (which is an Ohm's Law adaptation of Fick's First Law of Diffusion). It is easily shown that

$$g = \frac{A}{(c_a - p_i/p_t)} (0.23 + 1.37\omega) \quad (\text{A25})$$

where ω is the ratio of *total* and *stomatal* conductances to water vapour [$\omega = (1 + g \cdot r_{\text{bw}})^{-1}$]. Equations A25 and A15 represent independent constraints on g , and must be solved numerically. We solved the system by varying c_i upwards (starting at 1.1 p.p.m. above Γ^*) until the estimate of g from Eqn A15 was smaller than that from Eqn A25; at that point, the stepsize was halved and the direction of change in c_i was reversed. This procedure was repeated until the relative difference between the two estimates of g was less than 10^{-5} . When irradiance was below the light compensation point for photosynthesis [i.e. the value of I such that $J(I) < 4R_d(c_a + 2\Gamma^*)/(c_a - \Gamma^*)$] but above the irradiance causing stomatal opening (I such that $\alpha(I) > \gamma$), the sense of the algorithm must be reversed: c_i is varied upwards from $c_a + 1$ p.p.m., and reversed when g from Eqn A25 becomes smaller than that from Eqn A15. Finally, when I is sufficiently low that $\alpha(I) > \gamma$, we set $g = A = 0$ and $c_i = \Gamma = \Gamma^*(J + 8R_d)/(J - 4R_d)$. A user-friendly interface that solves the model is available as a downloadable executable file from the authors at <<http://bioweb.usu.edu/kmott/>>.

For the Monte Carlo simulations (Fig. 6j–o), response curves were obtained for each of a number of different simulated 'leaves' (six for Fig. 6j–l and 150 for Fig. 6m–o), in which several parameters were randomly varied using normal distributions (normal deviates were calculated as described by Press *et al.* 1992; pp. 289–290, using the random number generator described on p. 279 of the same text). Experimental estimates of the mean and SD were available for the parameters β , V_m , J_m/V_m , θ_j and F (see Table 1). For the parameters R , M , χ and π_c , we took the standard values (Table 1) to be the means of the parameter distributions, and we assumed coefficients of variation ($\text{CV} = \text{SD}/\text{mean}$) of either zero or 0.175; the latter value was the average CV among the five parameters in Table 1. Figure 6m–o present SD lines using both CV estimates for R , M , χ and π_c .

APPENDIX 4: PARAMETER ESTIMATION

Values for several parameters were estimated from previously published gas exchange and pressure probe measurements on *Vicia faba*. First, we fitted a floored plane

($a = \max\{c(P_g - \hat{m}P_e), 0\}$) by least-squares regression to the relationship between a , P_g and P_e given by Franks *et al.* (1998) for *V. faba* (using parameters for low P_e calculated by Buckley & Mott (2002a)), which yielded $c = 3.70 \mu\text{m MPa}^{-1}$ and $\hat{m} = 1.98$. This plane and the observed relationship to which it was fitted are shown in Fig. 9 and discussed in Appendix 1. Second, the aperture plane was combined with Eqns A1–A6 to yield a direct relationship between P_e and the product of aperture and D_s ($P_e = -aD_s[R\chi/c] + \psi_s + \pi_c$). Buckley & Mott (2002a) measured P_e , a and D_s concurrently by pressure probe and gas exchange, and reported a linear regression between P_e and aD_s with slope $-0.0013_1 \text{ MPa } \mu\text{m}^{-1} [\text{mmol H}_2\text{O mol}^{-1} \text{ air}]^{-1}$; this slope was used to calculate $R\chi/c$ and the product $R\chi$ ($0.0048 \text{ mol air mmol}^{-1} \text{ H}_2\text{O}$) was estimated by applying the value of c from the aperture plane. Third, R was estimated independently by Mott from measurements of transpiration rate and epidermal turgor pressure (submitted for publication) to be $0.045_6 \text{ MPa } [\text{mmol H}_2\text{O m}^{-2} \text{ s}^{-1}]^{-1}$, which puts χ at $0.10_5 \text{ mol air m}^{-2} \text{ s}^{-1} \text{ MPa}^{-1}$. Fourth, π_c was estimated as the intercept (0.52_5 MPa) of the P_e versus aD_s regression given by Buckley & Mott (2002a), assuming $\psi_s = 0$.

The parameters V_m , J_m , θ_j , F and β were estimated by gas exchange measurements on *V. faba* leaves (see Appendix 5 for gas exchange techniques) as follows. First, the initial slope of an A versus c_i curve was estimated by linear regression and applied to the derivative of Eqns A18 and A19 with respect to c_i to estimate V_m . Second, J was calculated from Eqns A18 and A20 using values for c_i and A measured at several values of incident irradiance, I , and these J -values were fitted by least-squares regression to Eqn A21 to estimate J_m , θ_j and F . Third, values of p_i measured by gas exchange at each of several different values of D_s were applied to Eqns A18–A23 to infer corresponding values of ATP concentration, τ . These were then applied to Eqn A15, together with the measured values of D_s , to estimate stomatal conductance, g ; the biochemical response parameter, β , was adjusted to produce the best fit of Eqn A15 to the values of g measured in the same gas exchange experiments. This entire procedure was repeated for five different leaves, each from a different individual, and the average of the five estimates for each parameter was used in the simulations. Table 1 gives the values estimated from each of the five different experiments.

APPENDIX 5: MATERIALS AND METHODS FOR GAS EXCHANGE MEASUREMENTS

Vicia faba L. plants were grown in 1 L pots containing equal parts peat moss, perlite and vermiculite. Plants were grown

in a controlled environment greenhouse with day and night temperatures of 30 and 20 °C, respectively, and day-length was extended to 16 h when necessary with high-pressure sodium lamps that provided a PFD of approximately $500 \mu\text{E m}^{-2} \text{ s}^{-1}$ at the top of the plant. Pots were drip watered to excess once a day with a nutrient solution containing 9.1 mM nitrogen, 1.8 mM phosphorus, 2.7 mM potassium and 11 μM chelated iron (Peter's 20–10220; Grace Sierra Horticultural Products, Milpitas, CA, USA).

Leaves were selected for uniformity of age and appearance. Gas exchange data were collected with a standard single-pass gas exchange system that has been described previously (e.g. Buckley & Mott 2000). N_2 , O_2 and CO_2 were mixed from pure compressed sources using mass flow controllers, and water vapour was added to the mixture by bubbling a portion the dry gas stream through degassed distilled water. The absolute concentration of O_2 in the mixture was measured with an O_2 electrode (Rank Brothers, Cambridge, UK); the absolute concentration of CO_2 was measured with an infrared gas analyser (ADC Mark III set in absolute mode; ADC, Hoddesdon, UK); and the absolute concentration of water vapour was calculated from the dewpoint of the mixture, which was measured with a chilled-mirror dewpoint hygrometer (Dew 10; General Eastern, Watertown, MA, USA). A portion of the gas flow was diverted for the reference cell of the differential infrared gas analyser (see below) and the rest was delivered to the leaf chamber. Flow rate to the chamber was measured with a mass flow meter. Gas returning from the chamber was picked up at ambient pressure and pumped through the analysis cell of a CO_2 and H_2O infrared gas analyser (LiCor 6262; LiCor Instruments, Lincoln, NE, USA). The gas in the leaf chamber was circulated by small rotary fans, and boundary layer conductance was $3.3 \text{ mol m}^{-2} \text{ s}^{-1}$. Leaf temperature was measured with a fine wire chromel–constantan thermocouple. Light was provided by a Xenon source and delivered to the leaf via a liquid light guide. Stomata were assumed to be in steady state when conductance did not change more than instrumental noise for 10 min. This often required an hour or more following a step change in environmental conditions.